수의학박사 학위논문

Enhanced gene therapy of lung and liver cancer by controlling autophagy and apoptosis

세포자식증 및 세포자살기전을 이용한 폐암 및 간암의 유전자치료 증진 연구

2013 년 2 월

서울대학교 대학원

수의학과 수의공중보건(수의독성학)전공

신 지 영

Enhanced gene therapy of lung and liver cancer by controlling autophagy and apoptosis

지도교수 조 명 행

이 논문을 수의학박사 학위논문으로 제출함
2012 년 11 월

서울대학교 대학원
수의학과 수의공중보건학(수의독성학) 전공
신 지 영

신지영의 수의학 박사 학위논문을 인준함
2012 년 12 월

위 원 장 한 호 재 (인)

부위원장 조 명 행 (인)

위 원 조 제 열 (인)

위 원 강 환 구 (인)

위 원 박 영 찬 (인)

ABSTRACT

Even with the development in medical technologies, lung and liver remained as difficult organs for early diagnosis for cancers. Therefore, morbidity and mortality figures still remain high. As cancer is not a disease cause by dysregulation of single gene or protein, it is hard to expect a complete recovery. Autophagy is a cellular mechanism controlling both cell survival and death. The thesis covers the therapeutic strategies to enhance the efficacy in aspects of controlling autophagy and introducing 2A peptide cleavage sequence to induce synergistic anti-tumor effects.

In Part I, beclin1 which plays a major role in autophagy has been chosen as a target. Beclin1 has been cloned into lentivirus vector and delivered to lungs of K-ras^{LA1} lung cancer model mouse twice a week for 4 weeks to induce prolonged activation of autophagy. As beclin1 has been delivered to the target organ, which is lung, beclin1, LC3-II levels have been increased and in turn, p62 has been decreased. Number and size of the tumors in the lungs of K-ras^{LA1} mice decreased after beclin1 delivery, and progression of tumorigenesis towards adenocarcinoma has been delayed in histopathological analysis. Under transmission electron microscopy, autophagic vacuoles have been detected as a typical outcome of autophagy activation, and add to the result, abnormal morphology of mitochondria has been detected. When apoptosis activates, nuclear changes come first and number of mitochondria increases as a compensatory mechanism. This phenomenon has been found in the lungs of K-ras^{LA1} mice after delivery of beclin1.

However, the amount of mitochondrial 12S RNA, which participates in generation of ATP in the mitochondria and counts as a standard of mitochondrial function, decreased after all. Mitochondria-related apoptotic proteins, Bax, Apaf-1, c-PARP and cytochrome, and TUNEL positive cells have been significantly increased. As a final consequence, not only autophagy, but also apoptosis were activated in lungs of K-ras^{LA1} mice.

In Part II, beclin1 was delivered to lungs of K-ras^{LA1} lung cancer model mice together with fractionated radiation to induce synergistic anti-tumor effect. Radiotherapy is known to induce radioresistance and to activate autophagy for cell survival. However, as proved in Part I, prolonged activation of autophagy can lead to autophagic cell death. Fractionated radiation opening to thorax (2 Gy, 5 times) to minimize the side effect and inhalation of beclin1 synergistically induced cancer cell death in lung cancers. Increase in number of autophagic vacuoles and increase in protein levels of beclin1, ATG5, LC3-II were observed. Radiation together with beclin1 inhalation activated the dissociation of beclin1-bcl2 complex and suppressed phosphorylation of Akt1 at Serine473 and Threonine308. It also affected both raptor in mTORC1 and rictor in mTORC2. Prolonged activation of autophagy induced positive feedback, suppressed Akt-mTOR pathway and maximized anti-cancer effects.

In Part III, 2A-peptide self-cleavage sequence was introduced to livers of H-ras12V liver cancer model mice, to activate two or more genes at the same time with equal efficiency. Using galactosylated-poly(ethylene glycol)-chitosan-graft-spermine (GPCS), which is a liver targeting non-viral vector, LETM1-2A-CTMP was made into complex and delivered to the target organ. After four weeks of

repeated exposures, 2A-peptide-mediated delivery was able to induce synergic effect of LETM1 and CTMP. The hepatocytes in the tumor area remained as altered foci, not being progressed as hepatocellular adenoma (HCA) or hepatocellular adenocarcinoma (HCC). Under transmission electron microscopy, the cristae of mitochondria have been disrupted and abnormal morphology in nuclear membrane (indentation and disruption of nuclear membrane) was observed. Protein levels of mitochondria-related apoptosis, including Apaf-1, bax and cytochrome *c*, as well as number of TUNEL positive cells were increased, confirming the activation of apoptosis in liver cancer.

Development of strategies minimizing side effects and maximizing therapeutic efficacy is important. Introduction of beclin1 to control autophagy and combination use of fractionated radiation proved to enhance the therapeutic efficacy. Also, linkage of LETM1 and CTMP using 2A peptide cleavage sequence induced synergistic outcome. Intervention of therapeutic mechanism which is known to bring side effects and introduction of techniques to control two or more genes are promising strategies to bring more effective outcome in development of gene therapeutics.

Keywords : Autophagy, Apoptosis, Lung cancer, Liver cancer, Gene Therapy

Student Number : 2009-31055

Contents

Abstract ..... **i**

Contents ..... **iv**

List of Figures ..... **vi**

List of Tables ..... **viii**

Backgound **1**

I. Overexpression of beclin1 induced autophagy and apoptosis in lungs of K-ras^{LA1} mice **7**

Abstract 8

Introduction 9

Materials and Methods 11

Results 15

Discussion 29

II. Aerosol delivery of beclin1 enhanced the anti-tumor effect of radiation in the lungs of K-ras^{LA1} mice **32**

Abstract 33

Introduction 34

Materials and Methods 36

Results 40

Discussion 55

III. Co-delivery of LETM1 and CTMP synergistically inhibits tumor growth in H-ras12V liver cancer model mice 60

Abstract 61

Introduction 62

Materials and Methods 64

Results 68

Discussion 92

Reference 97

국문초록 115

Publications 119

List of Figures

Figure 1. Transmission electron microscopy of A549, non small cell lung cancer (NSCLC) cell, after exposure to radiation (5Gy) 5

I. Overexpression of beclin1 induced autophagy and apoptosis in lungs of K-ras^{LA1} mice 7

Figure I-1. Delivery of Beclin1 to lungs of K-ras^{LA1} mice 16

Figure I-2. Gross morphology and histopathological analysis of tumors in lungs of K-ras^{LA1} mice 19

Figure I-3. Beclin1 induced mitochondria-related apoptosis in lungs of K-ras^{LA1} mice 22

Figure I-4. Analysis of proliferation and angiogenesis in lungs of K-ras^{LA1} mice 27

II. Aerosol delivery of beclin1 enhanced the anti-tumor effect of radiation in the lungs of K-ras^{LA1} mice 32

Figure II-1. Inhalation of beclin1 resulted in a synergistic anti-tumor effect with radiation in the lungs of K-ras^{LA1} mice 41

Figure II-2. Delivery of beclin1 via inhalation was successful and activated the autophagy pathway 45

Figure II-3. Radiation-stimulated dissociation of the beclin1-bcl2 complex and downregulation of Akt1-mTOR pathway in the lungs of K-ras^{LA1} mice.... 48

Figure II-4. Beclin1 with radiation decreased cell proliferation in lungs of K-ras^{LA1} mice 51

Figure II-5. Beclin1 with radiation decreased angiogenic activity in lungs of K-ras^{LA1} mice 54

III. Co-delivery of LETM1 and CTMP synergistically inhibits tumor growth in H-ras12V liver cancer model mice 60

Figure III-1. Delivery of GPCS/LETM1-2A-CTMP to livers of H-ras12V mice 69

Figure III-2. Gross morphology and histopathological analysis of tumors in livers of H-ras12V mice 72

Figure III-3. Mitochondria related apoptosis in livers of H-ras12V mice 75

Figure III-4. Synergistic anti-tumor effect via AMPK-AKT pathway in livers of H-ras12V mice 80

Figure III-5. Analysis of proliferation in livers of H-ras12V mice 84

Figure III-6. Analysis of angiogenesis in livers of H-ras12V mice 88

Figure III-7. Confirmation of H-ras12V used in the experiment 91

List of Tables

Table I-1. Summary of tumor incidence in the lungs of K-ras^{LA1} mice 20

Table II-1. Summary of tumor incidence in the lungs of K-ras^{LA1} mice 43

Table III-1. Summary of tumor incidence in the livers of H-ras12V mice 73

Background

Despite the development in science and advancement in technology, cancer remains as one of the incurable diseases which threaten the lives of people worldwide. Among various kinds of cancers, lung as well as liver is categorized as unapproachable organ which make it difficult to get diagnosed in early time period of cancer progression, therefore lowering the therapeutic efficacy.

Non-small cell lung cancer (NSCLC) is the most common type of lung cancer, accounting for 75–85%, of which only 15–25% of cases are potentially curable (RCR, 2006). Hepatocellular carcinoma (HCC) is the third-leading cause of death from cancer and the fifth most common malignancy worldwide (Thun *et al*., 2010). Highly active drug-metabolizing pathways and multidrug resistance transporter proteins in tumor cells further diminish the efficacy of current therapeutic regimens for HCC (Kota *et al*., 2009). Many efforts have focused on developing efficient therapeutics for lung and liver cancer; however, morbidity and mortality are still increasing constantly worldwide. Therefore, alternative approaches are needed to overcome these barriers to enhance therapeutic efficacy.

1. Apoptosis and Autophagy

Apoptosis is crucial in maintaining homeostasis in the adult organism, as in post-lactational mammary gland regression, ovarian follicular atresia and post-ovulatory regression, and in terminating an immune response by eliminating of activated

immune cells (Elmore, 2007). Dysregulation of apoptosis can result in the development of various pathologies. Insufficient apoptosis can lead to the development of cancer and autoimmune diseases. Excessive or inappropriate apoptosis, on the other hand, contributes to the injury that accompanies several diseases, such as neurodegenerative diseases and diabetes.

Autophagy is known as a third type of cell death, however, it is also a conserved catabolic process of cellular metabolism which functions as a survival mechanism (Debnath *et al*., 2005). Gaining of resistance to therapeutics, including chemical and radiation, makes it more difficult to enhance therapeutic efficacy. It has been suggested that survival mechanism of autophagy may play a role in gaining of resistance in cancer cells (Yang *et al*., 2011). At the same time, extensive autophagy is commonly observed in dying cells, leading to its classification as an alternative form of programmed cell death. The functional contribution of autophagy to cell death has been a subject of great controversy.

2. Viral and Non-Viral Vectors for Gene Delivery

Viral vectors consist of viral particles with nucleic acid covered by at least a capsid protein and an envelope. One or more viral structural genes are deleted to disable the spread of infectious particles into the hosts. Viral vectors typically contain strong and tissue specific promoters to support high level of transgene expression. For cancer gene therapy, viral vectors are widely in use – that it might be advantageous, since a prolonged host cell survival will also allow improved transgene expression and show better therapeutic efficacy (Lundstrom and

Boulikas, 2003).

Adeno-associated Virus (AAV) vectors are popular in gene therapy as it has broad range in transduction with a long-term expression mode (Rabinowitz and Samulski, 1998). The limited packaging capacity and the relatively inefficient large-scale production of AAV has restricted the use of these vectors to some extent. Other issues of concern for application of AAV are the preexisting immunity in humans to AAV and the random integration into the host genome.

Retrovirus has the capacity of integrating into the host cell genome and therefore provides long-term expression. Even with a broad range of hosts, retrovirus has a limitation in clinical use in that it fails to infect no-dividing cells such as neurons. However, modifications of the structures are still on process to overcome limitations and retrovirus vectors have been applied for cancer therapy (Huber *et al*., 1991; Roth *et al*., 1996) and bone marrow transplantation (Riviere *et al*., 1995).

Lentivirus belongs to the retrovirus family, but has some special features such as transduction of non-dividing cells. Many of the lentivirus vectors used in gene therapy applications are based on human immunodeficiency viruses (HIV).

Non-viral vectors, such as dendrimers, hyperbranched polymers and polymeric nanoparticles, are another choice for gene delivery. Cationic polymers form complexes with negatively charged DNA and targeting ligands, such as folate and galactose, may also be introduced on the surface of the dendrimers and hyperbranched polymers

Hyperbranched polymers differ from dendrimers in that they have less symmetric and polydispersity. The basic structure of hyperbranched polymers and

dendrimers consists of central core, the branching units and the terminal functional groups. The core together with the internal units determines the microenvironment of the nanocavities and, in turn, their solubilization properties, whereas the nature and the number of the external groups characterize their solubility, chemical and biological behavior.

Nanoparticles have been used in diversified ways to deliver drugs and genes into cells. When suitably encapsulated, a pharmaceutical can be delivered to the appropriate site, its concentration can be maintained at proper levels for long periods of time, and it can be prevented from undergoing premature degradation. Chitosan, a natural cationic polysaccharide, biodegradable poly (D,L-lactic acid) and poly(L-lysine)-graft-polysaccharide and thermosensitive copolymers based on poly(N-isopropylacrylamide) are under development (Alexandridou *et al*., 2001).

3. Enhancement of Efficiency in Gene Therapy

As cancer is not the disease which occurs with single gene dysregulation, there is a clear need for more complex designs of gene delivery system to target one or more genes at the same time with similar expression level. Designing of multicistronic vectors is the most crucial event to overcome the limitations of present technology.

Use of IRES (internal ribosomal entry sites) is the common way to express more than one protein in a single vector, however, the imbalance of protein expression makes it difficult to predict the level of expression of proteins and it is not easy to regulate the activity of the genes. As an alternative plan, 2A peptide cleavage sequences arise. It is noted for its small size and compare to IRES, it efficiently coexpresses genes that are placed between them (Furler *et al*., 2001;

Klump *et al*., 2001). The 'cleavage' occurs at the end of 2A peptide sequence with no need for additional factors such as proteases. After many trials with variety of protein functions and subcellular targeting, 2A peptide sequence is now in wide use for generating transgenic animals (Trichas *et al*., 2008). Boundless potential of 2A peptide in various diseases gives a chance to overcome the limitations of current gene therapy.

4. Thesis Overview

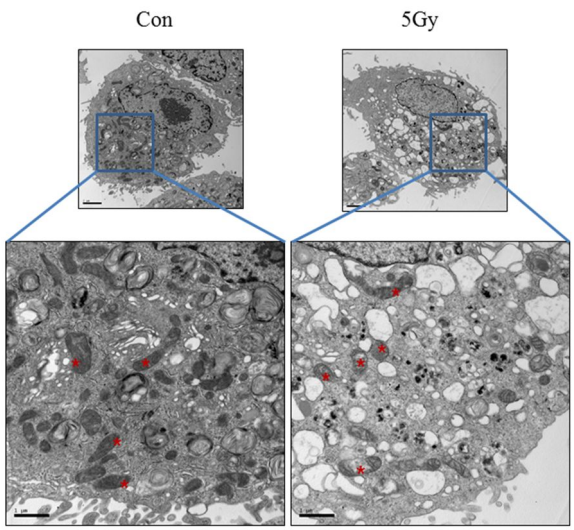

Figure 1. Transmission electron microscopy of A549, non small cell lung cancer (NSCLC) cell, after exposure to radiation (5Gy). Remarkable increase in autophagic vacuoles in cytoplasm, and defects in mitochondria were detected (Right Panel, Red asterisks). Blue boxes in the Top panel were magnified in Bottom Panel. Top. Magnification: x5000, Scale bar: 5 um. Bottom. Magnification: x50000, Scale bar; 0.5 um.

Experiments for Part I were conducted **to elucidate the role of autophagy and apoptosis in prolonged cancer therapy using beclin1 in vivo.** Radiotherapy, which is an avoidable choice of current cancer therapy, accompanies autophagy (Paglin *et al*., 2001) and mitochondrial defects (Figure 1) in preliminary study. The study covers the phenomenon after prolonged exposure of beclin1 to lungs of K-ras^{LA1} mice focusing on the morphological changes of nucleus and mitochondria.

Experiments for Part II were **conducted to see the synergic effect of radiotherapy and beclin1 in vivo.** Survival mechanism of autophagy activates with low dose of radiation, however, prolonged stimulus of autophagy with beclin1 overtakes to death mechanism, as well as signals of Akt1-mTOR-autophagy pathway.

Experiments for Part III were **conducted to see the dual targeting potential of 2A-peptide cleavage sequence with LETM1 and CTMP.** Both being the targets of mitochondria-related apoptosis, synergy effect of cell death mechanism was covered

Part I

Overexpression of beclin1 induced autophagy and apoptosis in lungs of K-ras^{LA1} mice

ABSTRACT

Beclin1, as a key molecule in controlling autophagy pathway, can activate both cell survival and cell death pathway. As role of autophagy in cancer progression remains controversial, introduction of Beclin1 to the lungs of K-ras^{LA1} mice was performed via inhalation. Prolonged autophagy activation was induced by repeated exposure of lentivirus-Beclin1, total of 8 times (2 times/week, 4 weeks). By the time of sacrifice, lungs were collected and analyzed for the therapeutic efficacy. Total number of tumors on surface and histopathological tumor progression were reduced in the lungs of K-ras^{LA1} mice. Successful delivery of Beclin1 induced autophagy and apoptosis in the target organ, which were confirmed by following features ; increased autophagic vacuoles in the cytosol, increased number of mitochondria with decreased mitochondrial 12S RNA, and increased protein levels of mitochondria-related apoptotis. Markers for cell proliferation and angiogenesis, which are used for prediction of cancer prognosis, were significantly reduced after introduction of Beclin1. Taken together, the results indicate that autophagy regulating gene, Beclin1, can be a potential target for lung cancer gene therapy.

1. INTRODUCTION

Lung cancer is the most common cause of cancer deaths worldwide, and the development of more effective therapy remains challenging (Parkin *et al*., 2001). Many efforts have focused on developing efficient therapeutics for lung cancer; however, morbidity and mortality are still increasing constantly worldwide.

Inhalation is promising in that it provides a route for non-invasive delivery of therapeutics directly to the lungs. Even with the limitations with biological barriers presented by the lung epithelium, inhalation has been proved its efficacy in treatment of cystic fibrosis (Alton *et al*., 1993) and lung cancer (Jiang *et al*., 2009; Yu *et al*., 2010) in mouse models.

Induction of cancer cell death is the key point in cancer therapy. Apoptosis is considered to be the only programmed cell death pathway, which is critical in tissue development and body maintenance. However, the phenomenon of autophagy arose as a second type of programmed cell death and it has received great attention in maintenance of homeostasis (Edinger *et al*., 2004; Lockshin *et al*., 2004).

Autophagy is an intracellular bulk degradation system, through which a portion of the cytoplasm is delivered to lysosomes to be degraded (Kuma *et al*., 2007). It is also known as a double-edged sword, in that it may play a role in cell survival and cell death (Shintani and Klionsky, 2004). Extensive autophagy is commonly observed in dying cells, leading to its classification as an alternative form of programmed cell death. However, the functional contribution of autophagy to cell death has been a subject of great controversy (Debnath *et al*., 2005). In 2007,

Yoshimori has suggested that uncontrolled and prolonged autophagy may activate cell death by degrading essential survival proteins or by degrading inhibitors of programmed cell death. Depending on the severity of stress or damage, the cells decide their fates – apoptosis, necrosis, autophagy or all at the same time (Lemasters *et al*., 1998).

This study covers the cellular events after prolonged activation of autophagy, induced by repeated exposure of beclin1 to the lungs of K-ras^{LA1} mice via inhalation. Focusing on the morphological changes in the cellular organelles proved that prolonged autophagy brings imbalance in homeostasis and damage mitochondria and nucleus which in turn activates mitochondria-related apoptosis.

2. MATERIALS AND METHODS

2.1. Materials

Antibodies against Beclin1, Bad, Bax, c-PARP, cytochrome C, phospho-Akt1 at Ser473, phospho-Akt1 at Thr308, PCNA, VEGF and b-actin were purchased from Santa Cruz Biotechnology (Santa Cruz, CA, USA). Monoclonal antibody against CTMP was produced following a general method described elsewhere (Hwang *et al*, 2007; Hwang *et al*., 2007, Hwang *et al*., 2009). Anti-Apaf-1, CD31 and p62 were obtained from Abcam (Beverly, MA, USA). Anti-phospho-AMPK at Thr172, AMPK and LC3 were purchased from Cell Signaling Technology (Boston, MA, USA). In Situ Cell Death Detection Kit was obtained from Roche Applied Science (Indianapolis, IN, USA)

2.2. Preparation and inhalation of lentivirus Beclin1

Full-length human BECN1 (GenBank ID: NM_003766) was subcloned into lentivirus entry vector (Invitrogen, Carlsbad, CA, USA) and transferred to lentivirus DEST vector (Invitrogen). Lentivirus-Beclin1 DEST vector was transfected to 293FT cells according to the manufacturer's protocols. Viral concentration was determined by HIV1 p24 ELISA kit (Perkin Elmer, Boston, MA, USA)

2.3. Animals

Male K-ras^{LA1} mice were obtained from the Human Cancer Consortium, National Cancer Institute Breeding Colony (Frederick, MD, USA) and maintained in a

laboratory animal facility with temperature and relative humidity maintained at 23 ± 2°C and 50 ± 20%, respectively, under a 12-h light/dark cycle. Twenty-one K-ras^{LA1} mice were randomly divided into three groups : Control, Vector Control and Beclin1. Animals were placed in a nose-only exposure chamber and nanosized lentivirus-Beclin1 particles were generated by patented nebulizer (Korea Patent #20304964). Total 30ml of lentivirus Beclin1 (concentration of 40 mg/ml) was exposed to animals for 30 minutes, twice a week for 4 weeks. All experimental protocols were reviewed and approved by the Animal Care and Use Committee of Seoul National University (SNU- 110809-4).

2.4. Quantitative polymerase chain reaction (RT-qPCR)

RNA was extracted from the lungs which were kept in RNA-later solution (Qiagen, Germantown, MD, USA). Amount of Mitochondrial 12S RNA was evaluated with following primers – GAPDH Forward : AACGACCCCTTCATT GAC, GAPDH Reverse : TCCACGACATACTCAGCAC, Mitochondria 12S RNA Forward : AACTCAAAGGACTTGGCGGTACTTTATATC, Mitochondria 12S RNA Reverse : GATGGCGGTATATAGGCTGAATTAGCAAGAG.

2.5. Electron microscopy

Lungs were fixed in modified Karnovsky's fixative before post-fixation in 1% osmium tetroxide in 0.05 M sodium cacodylate buffer (pH 7.2). Uranyl acetate (0.5%) was used for en bloc staining. The lungs were dehydrated in an ethanol series and embedded in Spurr's resin. Ultrathin sections were stained with 2% uranyl acetate and Reynolds' lead citrate and observed by TEM using an LIBRA

120 apparatus (Carl Zeiss, Oberkochen, Germany). Numbers of mitochondria were counted in 3 different fields of each slides.

2.6. Western blot analysis

Lungs were homogenized and protein concentrations were measured with a Bradford kit (Bio-Rad, Hercules, CA, USA). An equal amount of protein (30 ug) was loaded onto a sodium dodecyl sulfate (SDS) containing gel and separated. Primary and secondary antibodies conjugated with horseradish peroxidase (Invitrogen, Carlsbad, CA, USA) were applied according to the manufacturer's protocols. Bands of interest were obtained with an LAS-3000 luminescent image analyzer (Fujifilm, Tokyo, Japan).

2.7. Histopathological examination and immunohistochemistry (IHC)

Lung sections were prepared at a thickness of 4 um on charged slide glasses (Fisher Scientific, Pittsburgh, PA, USA). Slides were stained with hematoxylin and eosin for histopathological analysis. Sections were deparaffinized, rehydrated, antigens were retrieved and endogenous peroxidase was quenched for immunohistochemistry. Primary and secondary antibodies and 3,3'-diaminobenzidine (DAB) were applied accordingly (Vector Laboratories, Burlingame, CA, USA). Slides were reviewed using a light microscope (Carl Zeiss, Thornwood, NY, USA). Staining intensity was assessed by counting the number of positive cells in randomly selected fields viewed with appropriate magnification using In Studio version 3.01 (Pixera, San Jose, CA, USA).

2.8. Terminal transferase-biotin dUTP nick end labeling (TUNEL) assay

Sections were stained by In Situ Cell Death Detection Kit after deparaffinized by xylene, ethanol and then antigens were retrieved in 0.1M citrate buffer (pH6.0). Sections were then incubated in a humidified chamber at 37°C for 1 hour with TUNEL assay mixture containing TdT enzyme (TdT enzyme mediated digoxigenin-dUTP). Slides were washed with phosphate buffered saline (PBS), incubated with Converter-AP in humidified chamber for 30 min at room temperature and washed again. Another incubation with NBT/BCIP as a substrate for 10 min in dark, purple color was developed and examined under microscopy.

2.9. Statistical analysis

Quantification of Western blot analyses was performed with Multi-Gauge version 2.02 program (Fujifilm). All data are given as mean ± SE, and significant differences between groups were determined by unpaired t-test (Graphpad Software, San Diego, CA).

3. RESULTS

3.1. Delivery of Beclin1 to the lungs of K-ras^{LA1} via inhalation

Delivery of Beclin1 into the lungs of K-ras^{LA1} was successful, as shown in Figure I-1A. Total lysate of lungs were used to check expression of Beclin1-related proteins. Not only Beclin1, but also downstream molecules, LC3 and p62, were activated accordingly, which confirms the delivery of Beclin1 to successfully activate autophagy (Figure I-1A and 1B). Beclin1 normally expresses at the site of epithelial cells of bronchus. Overexpressed Beclin1 was confirmed with immunohistochemistry (Figure I-1C).

A

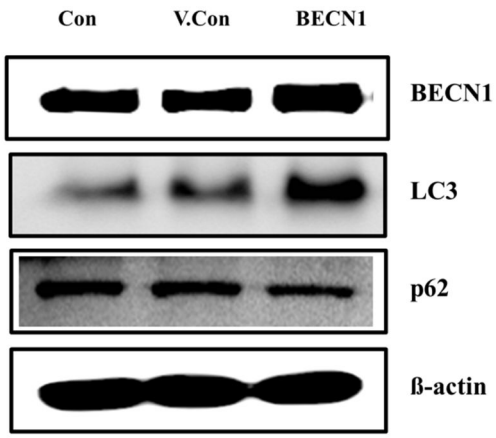
Con
V.Con
BECN1
BECN1
LC3
p62
ß-actin

B

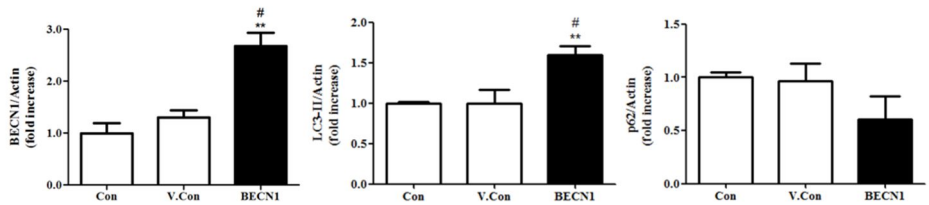
BECN1/Actin (fold increase)
3.0
2.0
1.0
0.0
#
**
Con
V.Con
BECN1
LC3-II/Actin (fold increase)
2.0
1.5
1.0
0.5
0.0
#
**
Con
V.Con
BECN1
p62/Actin (fold increase)
1.5
1.0
0.5
0.0
Con
V.Con
BECN1

C

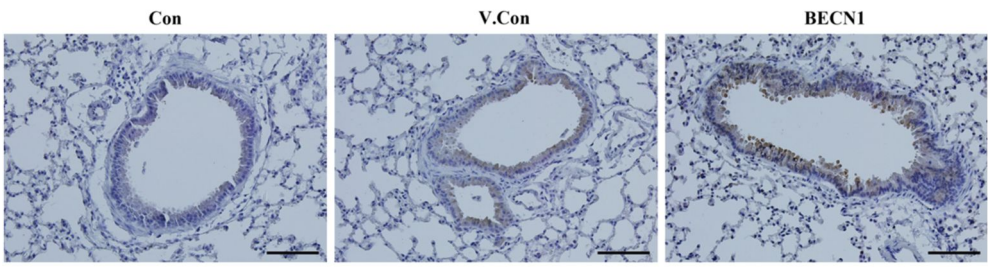
Con
V.Con
BECN1

Figure I-1. Delivery of Beclin1 to lungs of K-ras^{LA1} mice. A. Protein levels of Beclin1, LC3 and p62 were determined by Western blot. Bands are representative of five individuals from each group. **B.** Densitometirc analysis of Western blot. Each bar represents the mean±S.E (n=5). ** $p<0.01$ compared to Control. # $p<0.05$ compared to Vector Control. **C.** Delivery efficiency of beclin1 confirmed by immunohistochemistry. Magnification: x200. Scale bar: 20 um. Representative figures of five individuals from each group.

3.2. Therapeutic efficacy of Beclin1, inducing autophagy and apoptosis

The therapeutic capacity of Beclin1 was evaluated. K-ras^{LA1} mice start to develop lung cancer at the age of 5 weeks and cancer develops into adenocarcinoma. By the time of sacrifice, the mice were set to 12 weeks and the blockage of tumor formation was significant in Beclin1 treated group as shown in Figure I-2A. When total number of tumors were counted, measured and categorized into 2 groups according to their sizes (<1.0mm or >1.0mm), in Beclin1 treated group significantly showed decrease in both the number and size (Table I). The progression of lung cancer was examined histopathologically. The margin of tumor nodules was not clear, in other words, cancer cells were penetrated into normal tissue in invasive manner, however, well-demarcated margins with close-to-normal morphology of epithelial cells were observed in Beclin1 treated group (Figure I-2B). When histopathological grading was performed, the incidence or progression into adenocarcinoma was decreased. Overall therapeutic capacity of Beclin1 was summarized in Table I.

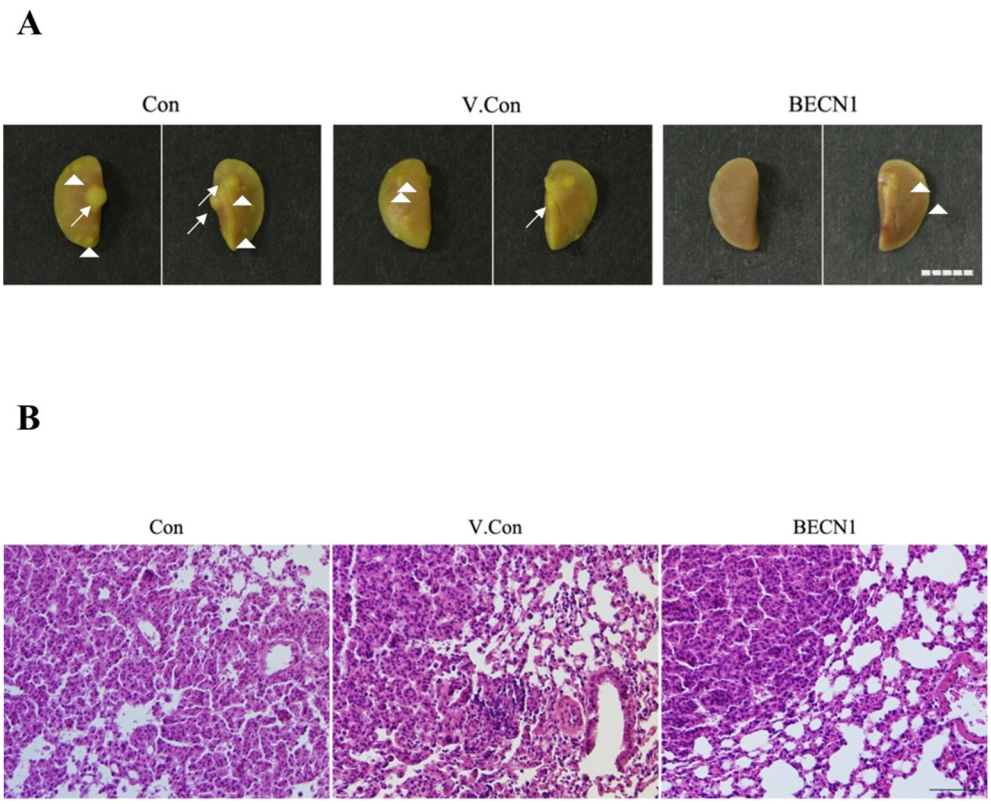

Figure I-2. Gross morphology and histopathological analysis of tumors in lungs of K-ras^{LA1} mice. A. Left lobes of the lungs were collected and fixed with 10% neutral formalin for the gross description of the tumors. Arrows indicate tumor size > 1.00mm. Arrowheads indicate tumor size < 1.00mm. Scale bar represents the actual size of 5 mm. **B.** Paraffin block of the lungs were sectioned at 3 um thickness for the histopathological analysis. Slides were stained with hematoxylin and eosin (H&E). Margin of the tumor and normal regions is presented with decreased pattern of invasiveness of tumors in beclin1-treated group. Magnification: x200. Scale bar: 20 um. Representative figures of five individuals from each group.

Table I. Summary of tumor incidence in the lungs of K-ras^{LA1} mice

Group	Number of Mice	Number of Tumors/ mouse			Adenocarcinoma	Adenoma [a]		
		Total	>1mm	<1mm		+++	++	+
Con	7	15.11±1.96	7.55±1.66	7.55±2.29	5	2	0	0
V.Con	7	13.89±3.60	5.94±1.70	8.11±3.15	6	0	1	0
BECN1	7	5.55±2.40***	2.50±1.69***	2.88±1.53***	2	0	4	1

Twenty-one K-ras^{LA1} lung cancer model mice were randonly divided into 3 groups ; Control, Vector Control, Beclin1. Animals were set to twelve weeks old by the time of sacrifice and lungs were collected at the ed of the experimental period. Tumors numbers were counted and size were measured with automated caliper. Incidence and multiplicity of lung proliferative lesions were compared (mean ± S.E.).

*** $p<0.005$ compared to Control group

a. Grades of adenoma ; +++ severe, ++ moderate, + mild

3.3. Mitochondrial changes in lungs of K-ras^{LA1} mice

Observation of autophagic vacuoles at the sites of tissue sections are definite evidence of autophagy. Each experimental group was put into transmission electron microscopy (TEM) analysis. Apart from the autophagic vacuoles in the section, surprisingly the changes in mitochondria and nucleus were evident (Figure I-3A). Nuclear membrane was disrupted and indentations in nucleus were prominent, which are representative features of apoptosis. Following the signs of apoptosis, the number and size of mitochondria increased with abnormal appearance – high density of contents in mitochondria and obscurity of cristae. Total numbers of mitochondria were counted and statistical analysis confirmed the increment with significance (Figure I-3B). Following the evidence that when mitochondrion lost its normal appearance, it may lose its function and homeostasis may go out of control. Level of mitochondrial 12S RNA, which is a determinant of mitochondrial function, was checked with quantitative real time PCR. Decrease in mitochondrial 12S RNA was prominent confirming that mitochondria were defective (Figure I-3C). Proteins which take parts in mitochondrial-related apoptosis pathway, such as Bad, Bax, Apaf-1, cleaved PARP and cytochrome *c*, increased as expectedly (Figure I-3D). Overexpressed cytochrome *c* release was further confirmed in tumor lesions of Beclin1 delivered mice (Figure I-3E). The cells undergoing apoptosis were examined by TUNEL assay (Figure I-3F) and counted accordingly (Figure I-3G), proving the high significance.

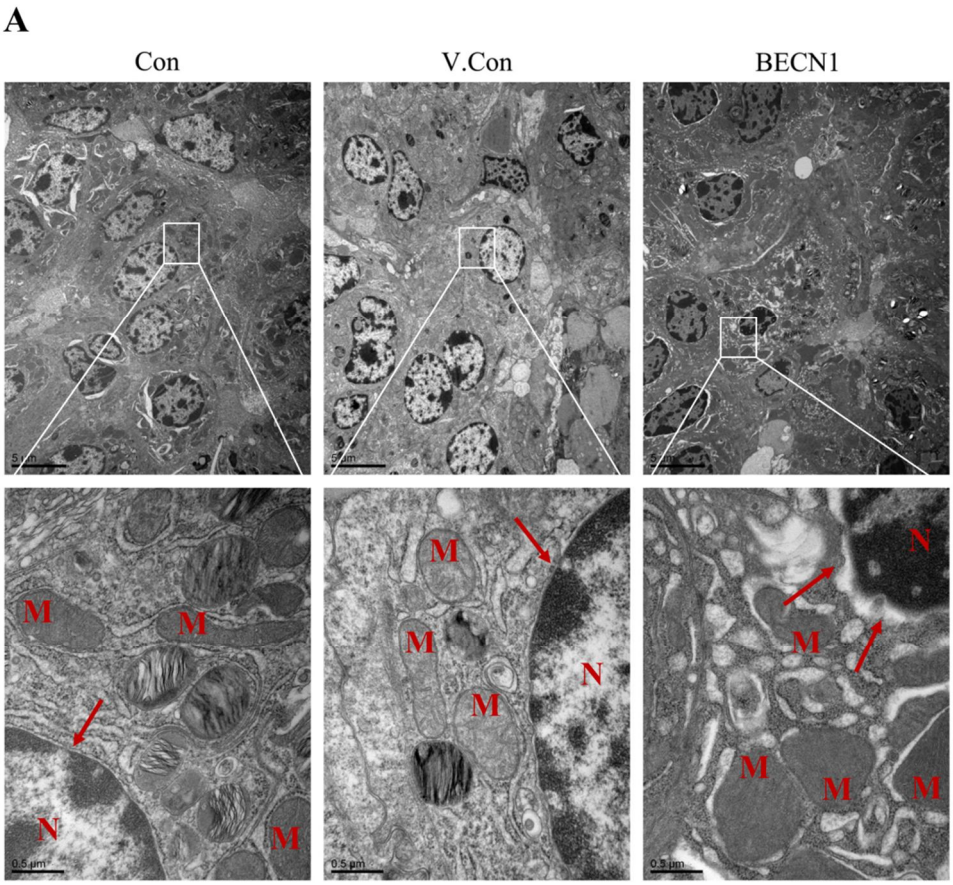
A
Con
V.Con
BECN1
M
N
0.5 μm
B
Number of Mitochondria (n)
30
20
10
0
##
**
Con
V.Con
BECN1

C

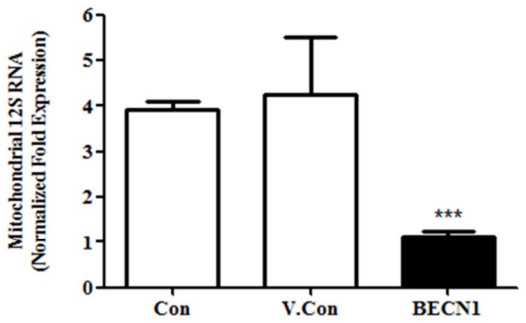
Mitochondrial 12S RNA
(Normalized Fold Expression)
6
5
4
3
2
1
0
***
Con
V.Con
BECN1

D

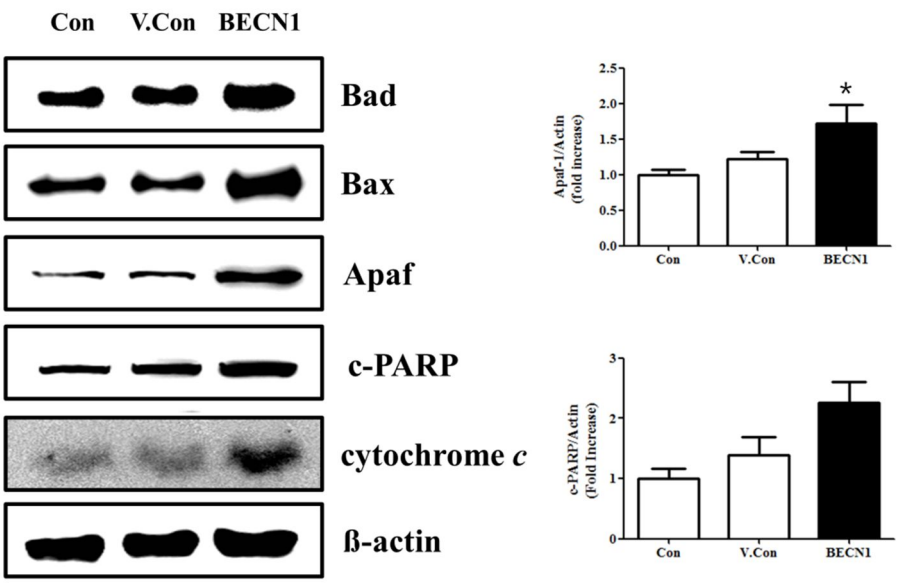
Con
V.Con
BECN1
Bad
Bax
Apaf
c-PARP
cytochrome c
ß-actin
Apaf-1/Actin
(fold increase)
2.5
2.0
1.5
1.0
0.5
0.0
*
Con
V.Con
BECN1
c-PARP/Actin
(Fold Increase)
3
2
1
0
Con
V.Con
BECN1

E

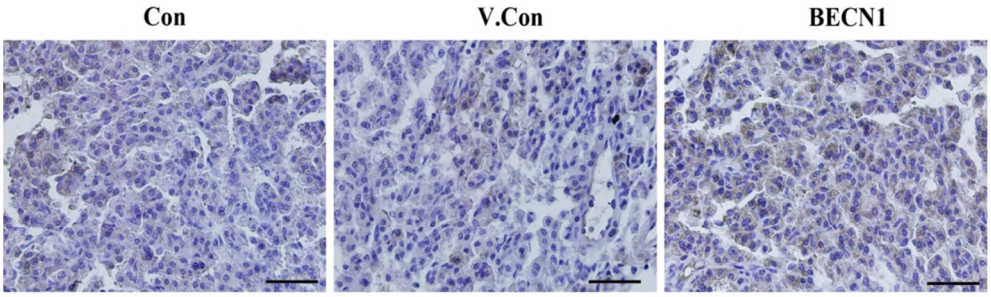
Con
V.Con
BECN1

F

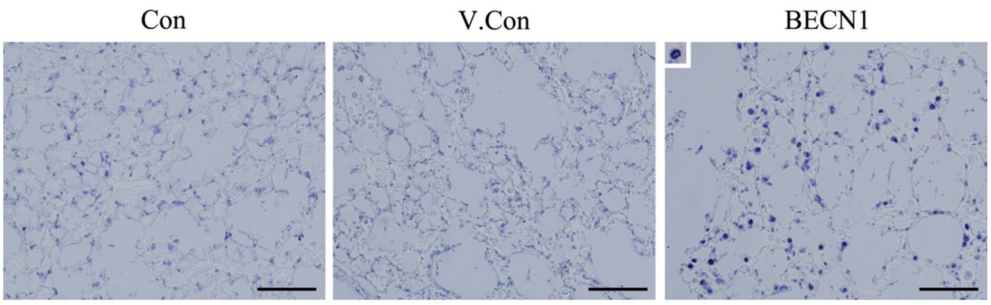
Con
V.Con
BECN1

G

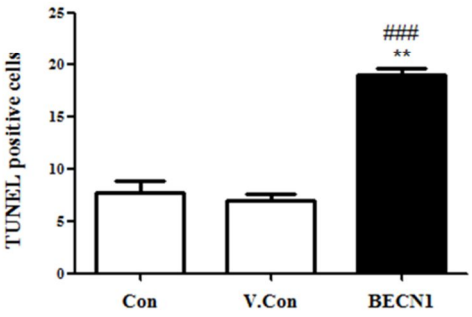
TUNEL positive cells
25
20
15
10
5
0
###
**
Con
V.Con
BECN1

Figure I-3. Beclin1 induced mitochondria-related apoptosis in lungs of K-ras^{LA1} mice. A. Transmission electron microscopy of tumors. White boxes in upper panel (Magnification: x5000, Scale bar: 5 um) were magnified in lower panel (Magnification: x50000, Scale bar: 0.5 um). Arrows indicate the margin of nucleus. N ; Nucleus, M ; Mitochondria. **B.** Numbers of mitochondria were counted in 3 different fields of each slide, and graphed accordingly. Each bar represents the mean±S.E (n=5). ** $p<0.01$ compared to Control, ## $p<0.01$ compared to Vector Control. **C.** Level of mitochondrial 12s RNA in lungs of K-ras^{LA1} mice was checked with RT-qPCR. Each bar represents the mean±S.E (n=5). *** $p<0.005$ compared to Control. **D.** Mitochondria-related apoptosis protein levels of Bad, Bax, Apaf-1, c-PARP and cytochrome *c* were determined by Western blot. Densitometric analysis of representative proteins, Apaf-1 and c-PARP, were presented. Each bar represents the mean±S.E (n=5). * $p<0.05$ compared to Control. **E.** Immunohistochemistry of cytochrome *c*. Magnification: x200. Scale bar: 20 um. Representative figures of five individuals from each group. **F.** TUNEL assay on tumor region. Magnification: x200. Scale bar: 20 um. Representative figures of five individuals from each group. **G.** TUNEL positive cells were counted and graphed. Each bar represents the mean±S.E (n=5). ** $p<0.01$ compared to Control, ### $p<0.005$ compared to Vector Control.

3.4. Decrease in proliferation and angiogenesis in lungs of K-ras^{LA1} mice

Prognosis of cancer can be determined by the ability of proliferation and angiogenesis. PCNA, which is a specific marker for proliferation that expresses only in the cells which undergo G1-S phase of cell cycle, was decreased in total lysate of the Beclin1 delivered lungs (Figure I-4A). Also PCNA positive cells in tumor lesions further confirmed the phenomenon of decrease in tumor cell proliferation (Figure I-4B and 4C). CD31 and VEGF, both the marker for angiogenesis were screened for evaluating angiogenic capability of Beclin1 delivered mice. Angiogenic capability also decreased in total lung lysate (Figure I-4A) and from immunohistochemical assay, the angiogenesis decreased both from the tumor and normal tissue of the lungs of K-ras^{LA1} (Figure I-4D).

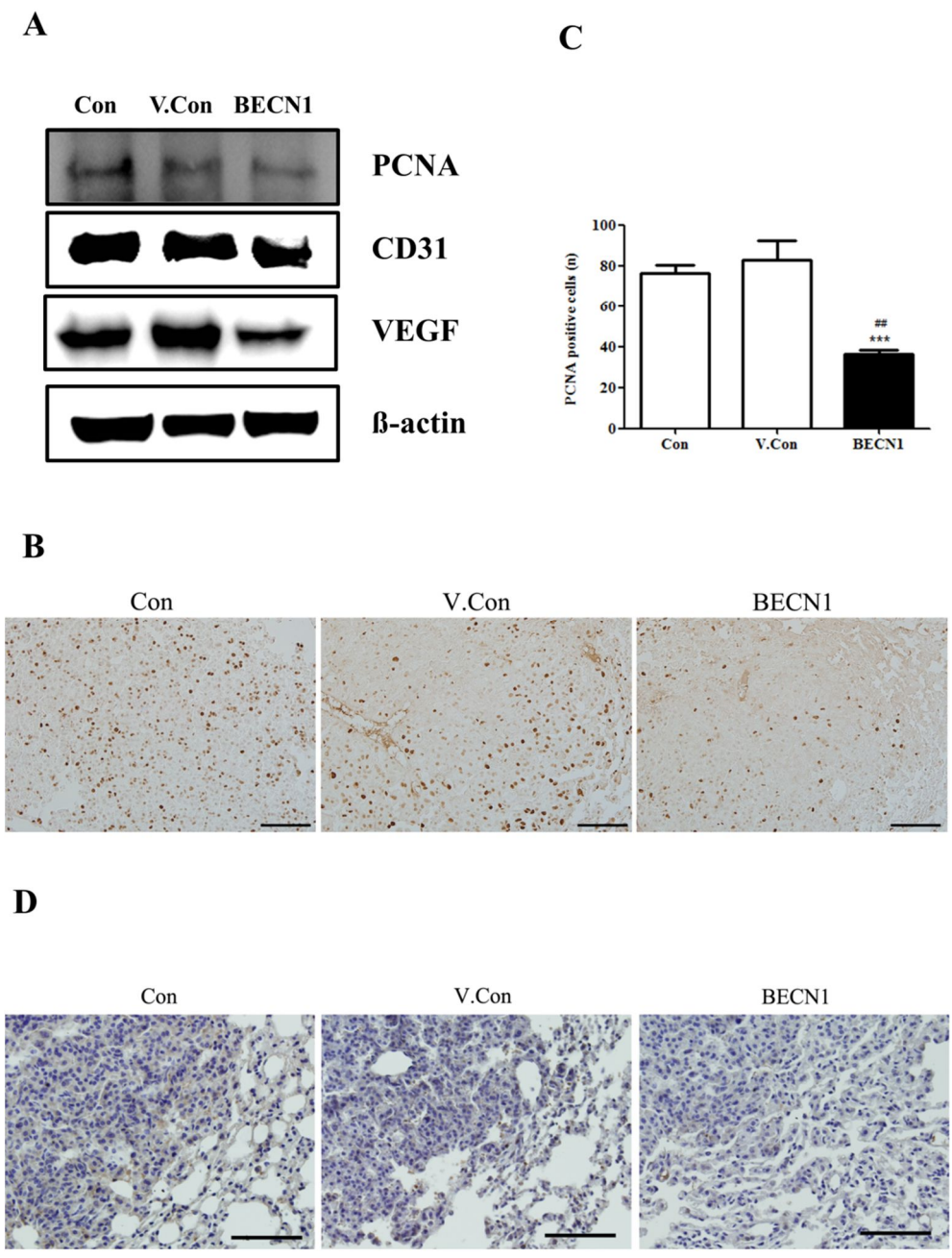
A
Con
V.Con
BECN1
PCNA
CD31
VEGF
ß-actin
C
PCNA positive cells (n)
100
80
60
40
20
0
##
***
Con
V.Con
BECN1
B
Con
V.Con
BECN1
D
Con
V.Con
BECN1

Figure I-4. Analysis of proliferation and angiogenesis in lungs of K-ras^{LA1} mice.

A. Protein level of PCNA , CD31 and VEGF were determined by Western blot. Representative bands of five individuals from each group. **B.** Immunohistochemisty of PCNA. Magnification: x200. Scale bar: 20 um. Representative figures of five individuals from each group. **C.** PCNA positive cells were counted and graphed. Each bar represents the mean±S.E (n=5). *** $p<0.005$ compared to Control, ## $p<0.01$ compared to Vector Control. **D.** Immunohistochemisty of CD31, counterstained with hematoxylin (nucleus). Magnification: x200. Scale bar: 20 um.

4. DISCUSSION

As the morbidity and mortality figures of lung cancer are increasing despite the advance in medical technology, development of novel approaches to overcome the limitation of existing therapeutic strategies is important. Recently autophagy, known to play a role in both cell survival and cell death, came up as a target mechanism for developing therapeutic regimens for metabolic diseases including neurodegenerative diseases and cancers (Kondo *et al*., 2005; Chen *et al*., 2011). However, it still remains controversial whether or not autophagy stimulates the process of tumor progression (Debnath *et al*., 2005).

Beclin1, being at the center of autophagy machinery, functions as a part of Class III PI3K/Vps34 complex (Rajawat *et al*., 2009). Even it is known as a tumor-suppressor, little is known about the mechanism by which Beclin1 functions in tumor suppression or about the interrelationship between its tumor suppressor and autophagy function (Furuya *et al*., 2005).

When Beclin1 was delivered to the lungs of K-ras^{LA1} mice via inhalation, continuous exposure to Beclin1 induced prolonged activation of autophagy pathway in the target organ. As autophagy is not a single time event but serial cellular events, delivering double-membraned vesicles to lysosome for degradation, levels of autophagy-related proteins may vary by the time of sacrifice, but still downstream proteins of Beclin1, such as LC3 and p62, remained activated. As a consequence of activated autophagy pathway, number of tumors and histopathological progression were regressed in the lungs of K-ras^{LA1} mice.

Accordance with the activation of autophagic proteins, excessive autophagic

vesicles were observed under transmission electron microscopy (TEM) images. At the same time, number of mitochondria was increased significantly as a sign of apoptosis (Schatten *et al*., 2001), compensating for the loss of survival cellular mechanism. As mitochondria are central components of cellular maintenance, many studies have been focused on exploring its mechanisms related to diseases directly related to energy metabolism, including cancers (Carew and Huang, 2002; Brandon *et al*., 2006). Even with the increased number of mitochondria, the nucleus of Beclin1 exposed groups showed the signs of apoptosis – prominent disruptions and indentations of the nuclear membrane (Parr *et al*., 1987; De Pol *et al*., 1997). Measuring the amount of mitochondrial 12S RNA can help to interpret the phenomenon, as it is the mitochondrial housekeeping gene and an indicator for functional mitochondria (Huang *et al*., 2004). Protein levels of Bad, Bax and Apaf-1, cleaved PARP and the release of apoptotic cytochrome *c* were increased simultaneously, which confirms the activation of mitochondria-related apoptosis**.** Bax is a proapoptotic protein that induces cell death by acting on mitochondria (Wolter *et al*., 1997; Marzo *et al*., 1998). Cytochrome *c* binding to Apaf-1, triggers caspase-3 dependent apoptosis pathway activation (Li *et al*., 1997; Perkins *et al*., 2000).

Cancer cell proliferation and neovascularization in the tumor sites are the features deciding the prognosis of cancer progression (Zhu *et al*., 2006). Doubling time of cancer cells is much shorter than normal ones and neovascularization cannot follow up the speed of cancer cell growth. However, as autophagy is known to activate under hypoxia or starvation conditions, it earns time for blood vessels to grow into the center of the tumors to proliferate. Therefore it is important to check

the prognosis markers for cell proliferation and angiogenesis after delivery of Beclin1. Proliferating cell nuclear antigen, PCNA, associates with cell cycle and specifically presents during G1-S phase. Vascular endothelial growth factor, VEGF, and CD31, also named as PECAM-1, is a positive marker for blood vessels. Significant decrease in protein levels confirmed Beclin1 as the potential therapeutic target for lung cancers.

Non-invasive approach using aerosol delivery helped to deliver the potential therapeutic gene, Beclin1, to the target organ. Introduction of Beclin1 to the lungs of K-ras^{LA1} mice positively regulated autophagy pathway to enhance the cell death mechanism. Inhibition of cell proliferation and neovascularization is a promising outcome for designing therapeutic regimen by controlling autophagy mechanism.

Part II

Aerosol delivery of beclin1 enhanced the anti-tumor effect of radiation in the lungs of K-ras^{LA1} mice

ABSTRACT

Radiotherapy alone has several limitations for treating lung cancer. Inhalation, a non-invasive approach for direct delivery of therapeutic agents to the lung, may help to enhance the therapeutic efficacy of radiation. Up-regulating beclin1, known as a tumor suppressor gene that plays a major role in autophagy, may sensitize tumors and lead to tumor regression in lungs of K-ras^{LA1} lung cancer model mice. To minimize the side-effects of radiotherapy, fractionated exposures (five times, 24-h interval) with low dose (2 Gy) of radiation to the restricted area (thorax, 2 cm) were conducted. After sensitizing the lungs with radiation, beclin1, complexed with a nano-sized biodegradable poly(ester amine), was prepared and delivered into the murine lung via aerosol three times/week for four weeks. In a histopathological analysis, animals treated with beclin1 and radiation showed highly significant tumor regression and low progression to adenocarcinoma. An increase in the number of autophagic vacuoles and secondary lysosomes was detected. Dissociation of beclin1-bcl2 stimulated autophagy activation and showed a synergistic anti-tumor effect by inhibiting the Akt-mTOR pathway, cell proliferation and angiogenesis. The combination of radiation with non-invasive aerosol delivery of beclin1 may provide a prospect for developing novel therapy regimens applicable in clinics.

1. INTRODUCTION

Lung cancer is one of the most life-threatening diseases. Non-small cell lung cancer (NSCLC) is the most common type of lung cancer, accounting for 75–85%, of which only 15–25% of cases are potentially curable (RCR, 2006). Many efforts have focused on developing efficient therapeutics for lung cancer; however, morbidity and mortality are still increasing constantly worldwide. Due to its anatomical structure and location, the lung has several limitations for an early diagnosis and surgical approach. Therefore, chemotherapy and/or radiation are compulsory treatments followed by surgical resection. Radiotherapy is the primary choice for inoperable NSCLC (stage I, II) or locally advanced disease (stage III). Various fractionation regimens and/or combination regimens with chemotherapy are on trial due to the poor outcome of high dose radiotherapy (Brady *et al*., 2005).

A non-invasive approach is under investigation to minimize the side-effects and maximize the efficacy of lung cancer treatment, and aerosol delivery of therapeutic agents directly to the target organ may be one of the most feasible candidates. However, several obstacles must be overcome to design an in vivo gene delivery study, including low delivery/expression efficiency, technical difficulties and organ-specific immune barriers. Previous studies have demonstrated the efficiency of gene delivery when complexed with non-viral or viral vectors through inhalation (Jin *et al*., 2008; Xu *et al*., 2008; Jiang *et al*., 2009) suggesting that aerosol gene delivery is plausible for clinical applications.

Beclin1 is a well-known tumor-suppressor gene, which plays a major role in autophagy, but is usually silenced in various cancers, including breast, cervical,

prostate and lung cancer (Pattingre *et al*., 2008; Sun *et al*., 2010). RNAi against beclin1 increases cell proliferation, and overexpressed beclin1 activates the autophagic death pathway (Wang *et al*., 2007). A recent study reported that beclin1 overexpression may up-regulate chemosensitivity, suggesting that beclin1 is a potent target for cancer gene therapy (Sun *et al*., 2010).

Here, the synergistic effect of a fractionated regimen of radiotherapy and beclin1 inhalation for tumor regression in the lungs of K-ras^{LA1} lung cancer model mice has been reported. Animals were divided into four groups: control, radiation, beclin1, combination of radiation and beclin1 – and therapeutic efficacies were determined and compared. Mice in the radiation only or beclin1 inhalation groups showed a decrease in tumor progression to some extent, whereas those in the combination treatment group showed a highly significant decrease. Consequently, the findings suggest that radiation with aerosol-delivered beclin1 may induce a synergic anti-tumor effect by controlling autophagic cell death via prolonged activation of autophagy. The overall results also suggest that combination gene therapy with radiation may be a good therapeutic strategy applicable in clinics.

2. MATERIALS AND METHODS

2.1. Construction of mTERT-beclin1 and preparation of the poly(ester amine)s/pDNA complex

The mouse TERT promoter sequence (GenBank: AF157502.1) was substituted into pcDNA3.1/CT-GFP-TOPO (Invitrogen, Carlsbad, CA, USA) with mouse beclin1, and the CMV promoter was removed from the BglII/KpnI enzyme sites. Poly(ester amine) was synthesized as described in a previous study, and a weight ratio of 1.3 was chosen (Arote *et al.*, 2007). Complexation of poly(ester amine)/pDNA was performed as described earlier and incubated at room temperature for 30 min before use.

2.2. Animals

Female K-ras^{LA1} mice (five mice/group) were obtained from the Human Cancer Consortium, National Cancer Institute Breeding Colony (Frederick, MD, USA) and maintained in a laboratory animal facility with temperature and relative humidity maintained at 23 ± 2°C and 50 ± 20%, respectively, under a 12-h light/dark cycle. All experimental protocols were reviewed and approved by the Animal Care and Use Committee of Seoul National University (SNU-201003-30).

2.3. Radiation and inhalation

Animals were anesthetized and immobilized in the treatment position for irradiation. Radiation was delivered at a dose rate of 1.85 Gy/min through a single posterior to anterior collimated 2-cm cobalt-60 beam with a 5-mm bolus placed

over the thoracic area. Mice were irradiated with 2-Gy fractions given over five consecutive days. To minimize the side-effects of radiation and to protect the salivary gland from radiation, only the thorax of the K-ras^{LA1} mice was exposed to 10-Gy radiation, fractionated five times at 24-h intervals (Albert *et al*., 2007; Kim *et al*, 2009; Moretti *et al*., 2009). Animals were placed into a nose-only exposure chamber for 30 min, and 1 mg plasmid DNA/BECN1 was delivered to the lungs via aerosol each time. Mice were sacrificed after four weeks (12 inhalations; three times/week for four weeks).

2.4. Electron microscopy

Lungs were fixed in modified Karnovsky's fixative before post-fixation in 1% osmium tetroxide in 0.05 M sodium cacodylate buffer (pH 7.2). Uranyl acetate (0.5%) was used for en bloc staining. The lungs were dehydrated in an ethanol series and embedded in Spurr's resin. Ultrathin sections were stained with 2% uranyl acetate and Reynolds' lead citrate and observed under transmission electron microscopy (TEM) (LIBRA 120, Carl Zeiss, Oberkochen, Germany).

2.5. Western blot analysis

Lungs were homogenized, and protein concentrations were measured with a Bradford kit (Bio-Rad, Hercules, CA, USA). An equal amount of protein (25 μg) was loaded onto a sodium dodecyl sulfate (SDS) gel and separated. Beclin1, p-Akt1 at Ser473, p-Akt1 at Thr308, vascular endothelial growth factor (VEGF), bcl-2, proliferating cell nuclear antigen (PCNA) and β-actin were purchased from Santa Cruz Biotechnology (Santa Cruz, CA, USA), Atg5 and LC3 were obtained

from Abgent (San Diego, CA, USA), Akt1 was purchased from Abfrontier (Seoul, South Korea) and p-mTOR, mTOR, raptor and rictor were purchased from Cell Signaling Technology (Danvers, MA, USA). Secondary antibodies conjugated with horseradish peroxidase (HRP) (Invitrogen) were applied according to the manufacturer's protocols. Bands of interest were obtained with an LAS-3000 luminescent image analyzer (Fujifilm, Tokyo, Japan).

2.6. Immunoprecipitation assay

Beclin1 and bcl-2 immunoprecipitation was conducted using Dynabead Protein G (Invitrogen), according to the manufacturer's protocol.

2.7. Histopathological examination and immunohistochemistry (IHC)

Lung sections were prepared at a thickness of 3 μm on charged slide glasses (Fisher Scientific, Pittsburgh, PA, USA). Slides were stained with hematoxylin and eosin (H&E) for histopathological analysis. Slides were deparaffinized, rehydrated, antigens were retrieved and endogenous peroxidase was quenched for immunohistochemistry. Primary and secondary antibodies and 3,3-Diaminobenzidine (DAB) were applied accordingly (Vector Laboratories, Burlingame, CA, USA). Slides were reviewed using a light microscope (Carl Zeiss, Thornwood, NY, USA). Staining intensity was assessed by counting the number of positive cells in randomly selected fields viewed with appropriate magnification using In Studio version 3.01 (Pixera, San Jose, CA, USA).

2.8. Statistical analysis

Quantification of Western blot analyses was performed with Multi-Gauge version 2.02 program (Fujifilm). All data are given as mean ± SE, and significant differences between groups were determined using Student's t-test (Graphpad Software, San Diego, CA, USA) .

3. RESULTS

3.1. Combination treatment decreased tumor incidence in the lungs of K-ras^{LA1} mice

Fractionated radiation alone did not decrease the number or size of tumor nodules compared with those in the control group; however, the changes were significant in the beclin1 and combination treatment groups (Table II, Figure II-1A). Lungs of the control group showed progressed adenocarcinoma with a dense population of tumor cells on H&E staining. However, adenocarcinomas were alleviated to adenomas in the radiation- and beclin1-treated groups, and near-normal structures of the lungs with a single lining of alveolar walls were observed in the combination treatment group (Figure II-1B). The overall anti-tumor effects of radiation and beclin1 are summarized in Table II.

A

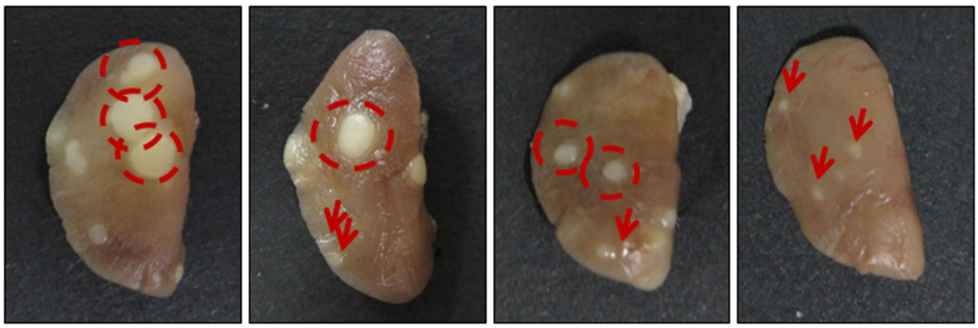

Control | Radiation Only | BECN1 Only | Radiation + BECN1

B

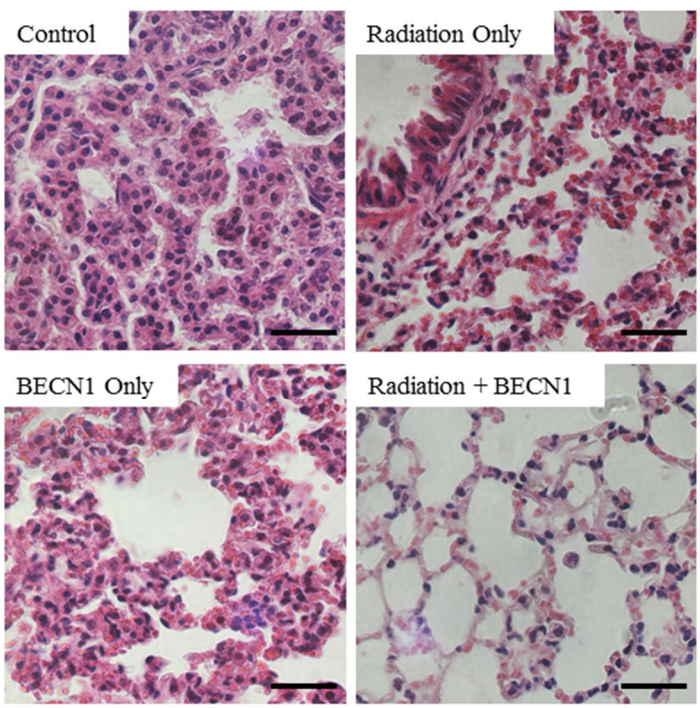

Figure II-1. Inhalation of beclin1 resulted in a synergistic anti-tumor effect with radiation in the lungs of K-ras^{LA1} mice. A Left lobes of the lungs were collected and fixed with 10% neutral formalin for the gross description of the tumors. Tumor nodules were counted, and sizes were measured with automated calipers. Dotted circles represent tumor nodules >1.0 mm. Arrows represent tumor nodules <1.0 mm. **B.** Lungs were paraffin-sectioned at 3 um for the histopathological description. Slides were stained with hematoxylin and eosin (H & E) for histopathological analysis. Magnification: ×400. Scale bar: 20 um. Representative figures of five mice per group

Table 2. Summary of tumor incidence in the lungs of K-ras^{LA1} mice

Group	Number of Mice	Number of Tumors / mouse			Adenocarcinoma	Adenoma[f]		
		Total	>1mm	<1mm		+++	++	+
Control	5	17.36±3.04	5.89±3.57	11.64±0.70	3	2	0	0
Radiation Only	5	16.44±2.71	5.28±2.72	10.92±3.83	2	0	1	2
BECN1 Only	5	11.19±1.21[a,c]	3.28±0.98	7.94±1.51	1	1	2	0
Radiation + BECN1	5	8.97±0.56[b,d,e]	2.92±1.10	6.06±1.61[b]	0	0	0	2

Twenty K-ras^{LA1} lung cancer model mice were randomly divided into 4 groups ; Control, Radiation Only, Beclin1 Only and Radiation / Beclin 1 Combination. Animals were set to seventeen weeks old by the time of sacrifice and lungs were collected at the end of the test period, the K-ras^{LA1} mice were killed, the lungs were collected, and the tumor numbers / sizes on the surface of lungs were counted. In parallel, the lungs from five mice were fixed in 10% neutral buffered formalin for histological examination. Incidence and multiplicity of lung proliferative lesions were compared. (mean±S.E)

a. $p<0.05$ compared to Control group

b. $p<0.01$ compared to Control group

c. $p<0.05$ compared to Radiation Only group

d. $p<0.01$ compared to Radiation Only group

e. $p<0.05$ compared to BECN1 Only group

f. Grades of adenoma ; +++ severe, ++ moderate, + mild

3.2. Aerosol delivery of beclin1 increased autophagy in the lungs of K-ras^{LA1} mice

Activation of the autophagy pathway was considered to examine the correlation between beclin1 and regression of tumor numbers. Intracellular lung tissue structures were observed under TEM. Various sizes of granules, which were considered normal, and primary lysosomes (arrows) were observed in the cytoplasm of cells from the control and radiation groups (Figure II-2A). An increase in the number of vacuoles in the cytoplasm (arrow heads) was distinguishable in the beclin1 group. In particular, the combination treatment group showed many secondary lysosomes (circle heads) indicating autophagosomes fused with lysosomes (Figure II-2A). Western blots were performed to further confirm the activation of autophagy-related proteins. As a result, an increase in beclin1, ATG5 and LC3-II was detected (Figure II-2B), and densitometry analysis of beclin1 supported these findings accordingly (Figure II-2C). Efficiency of beclin1 inhalation was further confirmed with IHC and epithelial cells of the bronchioles showed marked increase, especially in the beclin1- and combination-treated groups (Figure II-2D).

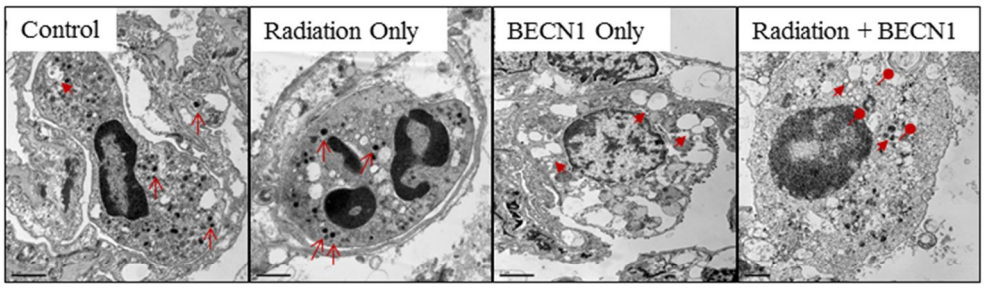
A
Control
Radiation Only
BECN1 Only
Radiation + BECN1

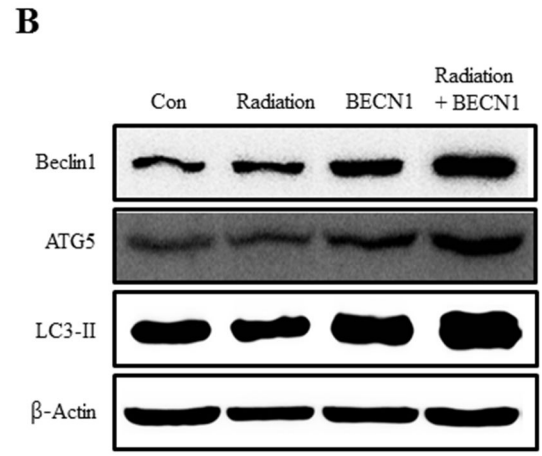
B
Con
Radiation
BECN1
Radiation + BECN1
Beclin1
ATG5
LC3-II
β-Actin

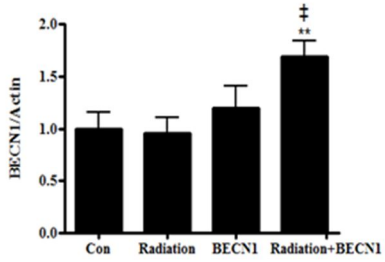
C
BECN1/Actin
2.0
1.5
1.0
0.5
0.0
‡
**
Con
Radiation
BECN1
Radiation+BECN1

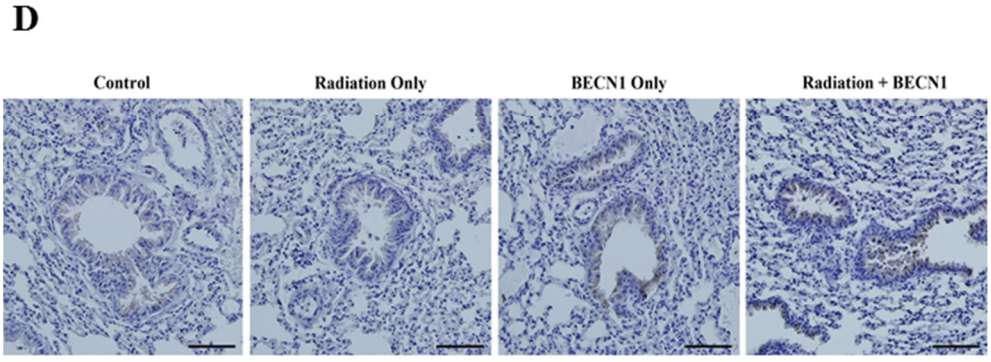
D
Control
Radiation Only
BECN1 Only
Radiation + BECN1

Figure II-2. Delivery of beclin1 via inhalation was successful and activated the autophagy pathway. A. Intracellular lung structures were screened under transmission electron microscopy. Arrows, primary lysosomes; Arrow-heads, cytoplasmic vacuoles; Circle-heads, secondary lysosomes/ autophagolysosomes. Magnification: ×6000. Scale bar: 1 um. **B.** Western blot was performed to monitor the increase in autophagy-related proteins: beclin, ATG5, and LC3. Bands are representative of five individuals from each group. **C.** Densitometric analyses reconfirmed the synergistic effect of beclin1 on autophagy. Each bar represents the mean ± S.E. (n = 5). **$p < 0.05$ was considered highly significant compared to the control group and ‡$p < 0.01$ was highly significant compared to the radiation group. **D.** Delivery of beclin1 and its synergistic effect in combination group were confirmed with immunohistochemisty analysis; beclin1. Magnification: x200. Scale bar: 20 um Representative figures of five mice per group.

3.3. Combination treatment increased the dissociation of the beclin1–bcl2 complex and down-regulated the Akt1–mTOR pathway

As beclin1 is a binding partner of bcl2, binding affinity is considered important to maintain the cellular regulation. Dissociation of the beclin1–bcl2 complex is a compulsory event before activating the autophagy pathway (Liang *et al*., 2006; Wei *et al*., 2008; Ciechomska *et al*., 2009; Zalckvar *et al*., 2009). An immunoprecipitation assay with beclin1 and bcl2 antibodies was performed to determine the extent of dissociation of this complex. The combination treatment showed a definite decrease on sodium dodecyl sulfate-polyacrylamide gel electrophoresis (SDS-PAGE), confirming less binding affinity of these two proteins (Figure II-3A).

Akt1 and mTOR phosphorylation is associated with tumor formation and progression (Choe *et al*., 2003), and mTOR has a direct effect on the autophagy pathway (Maiuri *et al*., 2007; Jung *et al*., 2009; Brech *et al*., 2009; Jung *et al*., 2010). Akt1 is a serine/threonine protein kinase that plays a major role in cell growth, proliferation and survival. The treated groups, particularly the combination treatment group, showed a decrease in both Akt1 phosphorylation sites (Ser473 and Thr308), demonstrating that the anti-tumor effect was activated by suppressing the Akt1 pathway (Figure II-3B). Furthermore, the mTOR and phospho-mTOR expression levels were suppressed. The protein levels of raptor and rictor as a part of mTORC1 and mTORC2, respectively, were also decreased by both the beclin1 and combination treatments (Figure II-3C).

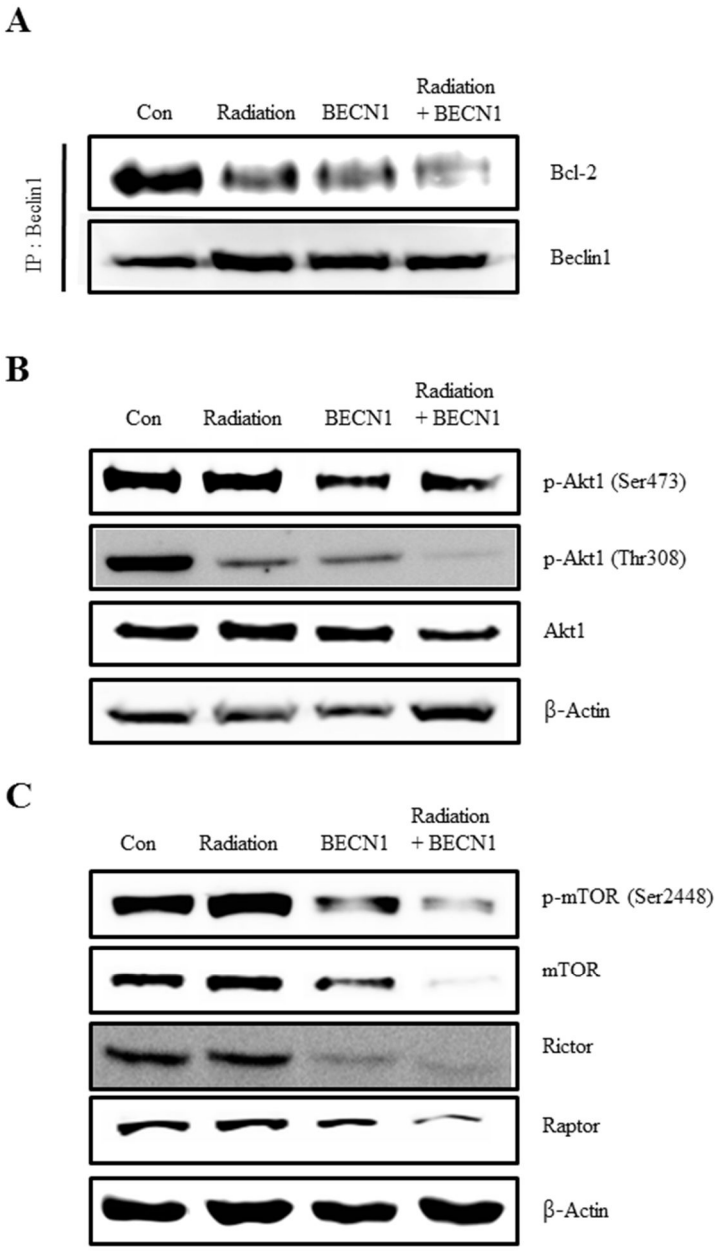
A
Con
Radiation
BECN1
Radiation + BECN1
IP : Beclin1
Bcl-2
Beclin1
B
Con
Radiation
BECN1
Radiation + BECN1
p-Akt1 (Ser473)
p-Akt1 (Thr308)
Akt1
β-Actin
C
Con
Radiation
BECN1
Radiation + BECN1
p-mTOR (Ser2448)
mTOR
Rictor
Raptor
β-Actin

Figure II-3. Radiation-stimulated dissociation of the beclin1-bcl2 complex and downregulation of Akt1-mTOR pathway in the lungs of K-ras^{LA1} mice. A. SDS-PAGE of the beclin1 and bcl2 lung lysate immunoprecipitation. IP beads were bound to the beclin1 antibody and immunoblotted with the bcl2 antibody. **B.** Western blot analysis using phospho-Akt1 at Thr308, phospho-Akt1 at Ser473, and Akt1. **C.** Western blot analysis with phospho-mTOR at Ser2448, mTOR, raptor, and rictor antibodies. Bands are representative of five individuals from each group.

3.4. Combination treatment decreased cell proliferation in the lungs of K-ras^{LA1} mice

PCNA was selected as a marker and a western blot was performed to examine the correlation between tumor regression and cell proliferation. The combination treatment group showed a highly significant decrease in proliferation, whereas beclin1 alone also showed an anti-proliferative effect to some extent, compared with that in the radiation and control groups (Figure II-4A). The IHC analysis further confirmed the anti-proliferative effect of the combination treatment (Figure II-4B and 4C).

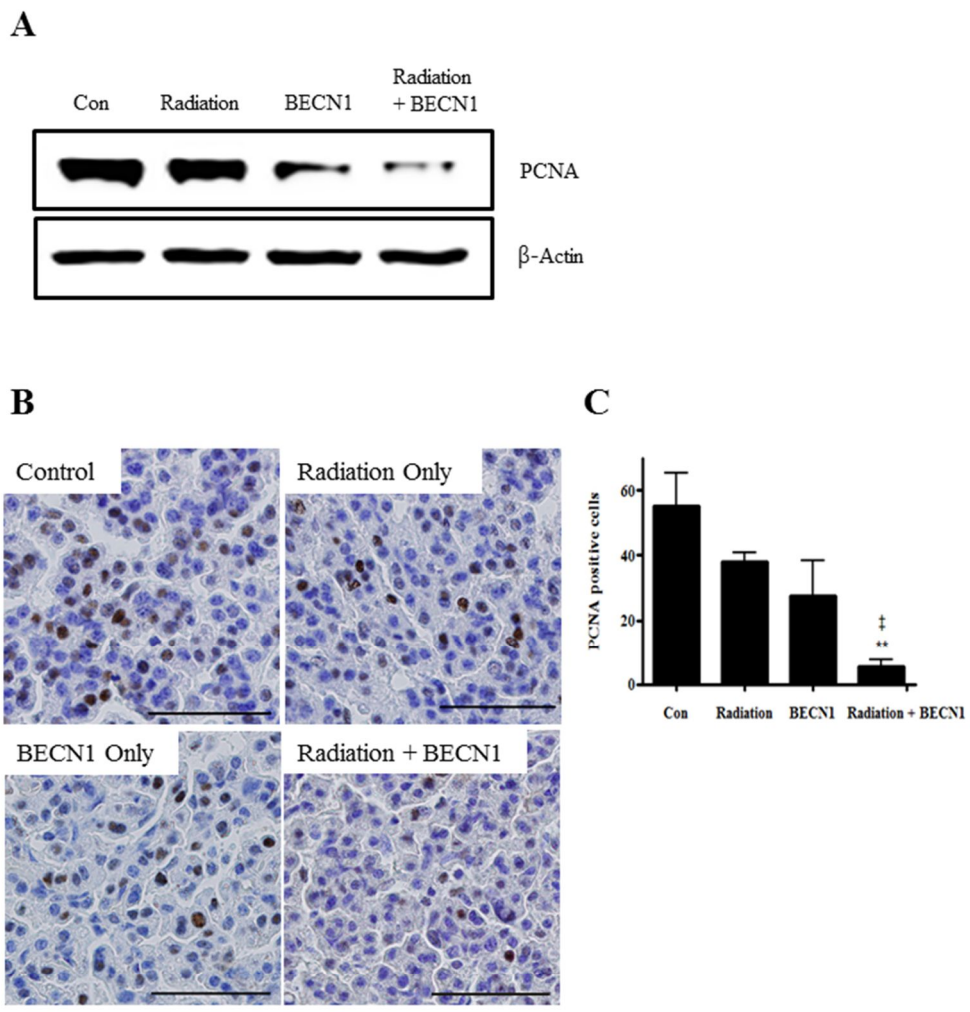
A
Con
Radiation
BECN1
Radiation + BECN1
PCNA
β-Actin
B
Control
Radiation Only
BECN1 Only
Radiation + BECN1
C
PCNA positive cells
60
40
20
0
‡
**
Con
Radiation
BECN1
Radiation + BECN1

Figure II-4. Beclin1 with radiation decreased cell proliferation in lungs of K-ras^{LA1} mice. A. Western blot of anti-PCNA and the total lung tissue lysates. Bands are representative of five individuals from each group. **B.** The immunohistochemistry analysis showed fewer double stained nuclei with hematoxylin and chromogen on lung tissue slides. Magnification: ×400. Scale bar: 50 um. **C.** Statistical analysis of PCNA positive cells. Nuclei double-stained with DAB and hematoxylin were counted in three different fields from each slide. Each bar represents the mean ± S.E. (n = 5). **p < 0.01 was considered highly significant compared to the control group. ‡p < 0.01 was considered highly significant compared to the radiation group. Representative figures of five mice per group.

3.5. Combination treatment inhibited angiogenesis in lungs of K-ras^{LA1} mice

Angiogenesis, the ability to build new blood vessels, is a vital process for tumor growth. VEGF-A, the pro-angiogenic marker, was selected to determine the extent of angiogenesis at the target site. The radiation group did not show a significant change compared with that in the control; however, a decreased protein level was detected in the beclin1 group and a further decrease was observed in the combination treatment group (Figure II-5A). Decreased VEGF-A expression in the combination treatment group was also demonstrated by IHC (Figure II-5B).

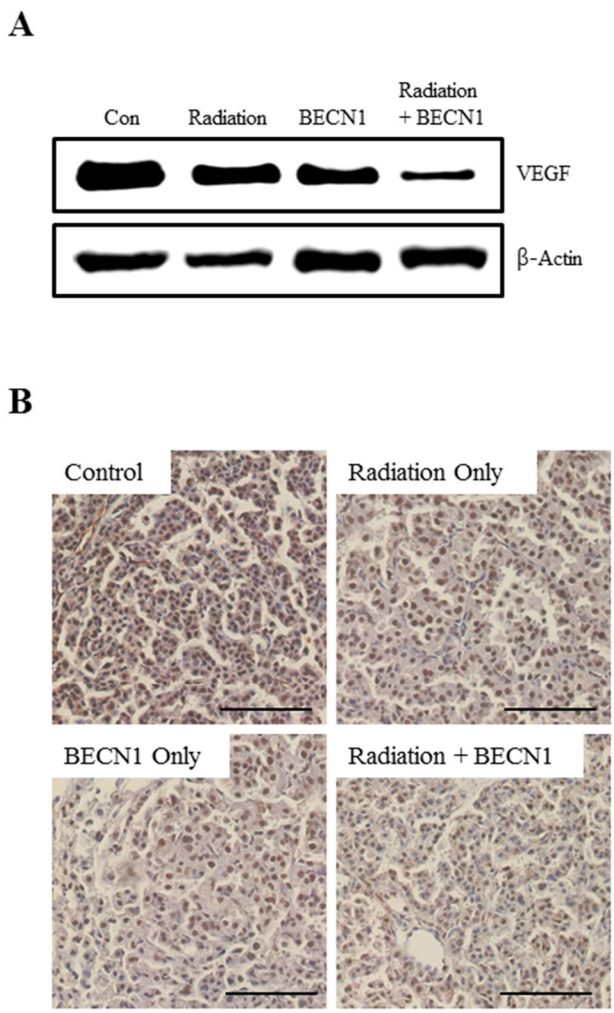

Figure II-5. Beclin1 with radiation decreased angiogenic activity in lungs of K-ras^{LA1} mice. A. Western blot analysis using total lung tissue lysates and anti-VEGF. Bands are representative of five individuals from each group. **B.** The immunohistochemistry analysis showed less chromogen expression in the combination treatment group, confirming A. Magnification: ×200. Scale bar: 10 um. Representative figures of five mice per group.

4. DISCUSSION

Radiation therapy has been applied widely, despite the fact that high dose radiation leads to systemic side-effects. Therefore, in this study, fractionated radiotherapy to the thorax of K-ras^{LA1} mice to maximize the therapeutic effects with fewer side-effects has been reported. Various kinds of vectors have been developed to deliver specific genes to target organs, and various routes of delivery have been studied (Dachs *et al*. 1997; Li *et al*., 2000). In this study, poly(ester)-amine, a modified non-viral vector based on branched polyethyleneimine was used. Previous study has proved the carrier has significantly low cytotoxicity with high transfection efficiency (Arote *et al*., 2007). Fractionated radiation did not result in significant therapeutic effects, as summarized in Figure II-1 and Table II. Showing no significant difference from the control group, it can be assumed that mice treated with a low dose of radiation have recovered from the autophagic stress by the time of sacrifice. Interestingly, beclin1 alone seemed to have a therapeutic effect to some extent; however, the combination treatment resulted in highly significant tumor regression. Therefore, a combination radiotherapy treatment may allow for more effective outcomes. In fact, the overall results are supported by recent studies indicating that radiation with chemotherapeutics or other agents increases the effects of radiotherapy alone (Adams *et al*., 1984; Lawrence *et al*., 1996; Kim *et al*., 2008).

The autophagy pathway is a catabolic intracellular process that activates the lysosomal degradation pathway. During autophagy, cytoplasmic structures are sequestered into double-membraned or multi-layered autophagosomes and fused

with lysosomes to form secondary lysosomes or autophagolysosomes for degradation (Shintani *et al*., 2004). In addition to the formation of various density-graded granules in the cytoplasm of lung tissues, an increased number of vacuoles were observed both in the beclin1-delivered and combination treatment groups. Moreover, the beclin1-delivered group showed more secondary lysosomes than primary lysosomes compared with the control and radiation groups, whereas the combination treatment group showed many multi-layered structures and autophago-lysosomes (Figure II-2A). Protein expression levels further supported the TEM analysis in that autophagy-related proteins were overexpressed in the beclin1-delivered group, particularly a highly significant increase was observed in the combination treatment group (Figure II-2B and 2C). Interestingly, fractionated radiation itself did not show marked autophagy activation in vivo and beclin1 alone activated autophagy pathway, and the combination therapy further stimulated the beclin1 pathway leading to autophagic cell death. IHC of beclin1 in the lungs confirmed the synergistic effect of beclin1 expression (Figure II-2D). Autophagy is still controversial in that it may promote tumor cell survival, as activated autophagy can be detected under hypoxic or starved conditions of the tumor microenvironment. However, autophagy as a survival mechanism only lasts for a limited time, and prolonged autophagy leads to cell death (Yang *et al*., 2011; Azad *et al*., 2008). The results are supported by recent studies indicating that activation of the autophagy pathway is correlated with tumor regression (Pouyssegur *et al*., 2006; Maiuri *et al*., 2008; Gozuacik *et al*., 2004).

As beclin1 is a binding partner of bcl2, binding affinity is considered important to maintain the cellular regulation. According to previous findings, low levels of

beclin1 reduce its capacity to activate autophagy (Ciechomska *et al*., 2009; Liang *et al*., 2006) and under stress conditions, such as hypoxia or starvation, which activate autophagy, beclin1 dissociates from the complex for activation (Wei *et al*., 2008). Activating autophagy with radiation and beclin1, binding affinity of beclin1-bcl2 decreased significantly (Figure II-3A). A recent study revealed that activating autophagy induces phosphorylation of beclin1 to stimulate dissociation of beclin1-bcl2 complex (Zalckvar *et al*., 2009).

Akt1 and mTOR phosphorylation is strongly correlated with tumorigenesis and tumor progression (Choe *et al*., 2003). In particular, mTOR has a direct effect on the autophagy pathway (Maiuri *et al*., 2007; Jung *et al*., 2009; Brech *et al*., 2009; Jung *et al*., 2010). Many studies have been conducted with mTOR inhibitors to induce autophagy to confirm anti-tumor effects, but not with direct targeting of the autophagy pathway. Radiation with beclin1 was a novel approach and proved that it showed similar effects to using mTOR inhibitors (Figure II-3B and 3C). Akt1 is important in most cellular events (Xu *et al*., 2010), and phosphorylation at both serine473 and threonine308 must occur for full Akt1 activation (Fujita *et al*., 2002; Hait *et al*., 2006). A decrease in phosphorylation at both sites was observed in the beclin1-delivered groups, and the combination treatment group showed a highly significant decrease in phosphorylation at Thr308 and Ser473 (Figure II-3B). Thus, cellular fate induced by beclin1 and/or the combination treatment may be significantly different from that in control cells. The results can be supported by recent studies reporting that different rates of phosphorylation are dependent on the cellular environment (Chen *et al*., 2001). Even the radiation-only group did not show any significant difference in the Akt–mTOR pathway, but interestingly with

beclin1 it definitely down-regulated Akt-mTOR signaling. Radiation has been studied to effect mTORC2-Akt, which is upstream of Akt-mTORC1 (Tanaka *et al*., 2011), and combination therapy showed marked suppression of both mTOR complexes. mTOR can be divided into mTORC1 with raptor and mTORC2 with rictor. Delivery of beclin1 affected both complexes, as well as mTOR phosphorylation itself (Figure II-3C), and the combination treatment induced a further decrease. Several lines of evidence have demonstrated that mTORC2 directly phosphorylates Akt1 at Ser473 and facilitates PDK1-mediated Akt1 phosphorylation at Thr308 (Sarbassov *et al*., 2005). Drugs targeting mTOR complexes, such as rapamycin derivatives, potently inhibit Akt1 activity in cancer cells by suppressing mTORC2 and the mTORC1 pathway followed by down-regulation of p70S6K and 4EBP1 phosphorylation (Zeng *et al*., 2007). These findings fit well with the results, because the combination treatment resulted in significant tumor regression by affecting the Akt1 pathway, leading to mTORC1 and mTORC2 down-regulation.

Cell proliferation and angiogenesis are markers to predict the fate of tumorigenesis (Gasparini and Harris, 1995; Phillips *et al*., 2006). Cancers have a tendency to grow quickly and may metastasize to other organs. Therefore, checkpoints to anticipate the prognosis of tumors are PCNA for proliferation and VEGF-A for angiogenesis (Maeda *et al*., 2000; Sui *et al*., 2002) in the tumor regions. Overexpression of PCNA and VEGF have been observed in various human tumors; therefore, they are used as biomarkers of invasiveness, vascular density, metastasis and recurrence (Dvorak, 2002; Ferrara, 2004). The results also demonstrated that a decrease in PCNA and VEGF-A was well correlated with

tumor regression concurrent with a decrease in angiogenesis and cell proliferation at the tumor regions (Figure II-4 and II-5). It suggests that the combination treatment effectively regressed tumors by inhibiting cancer cell metastasis, proliferation and angiogenesis.

In summary, it has been demonstrated in this study that the combination treatment was more effective for treating lung cancer compared with fractionated radiation or beclin1 delivery. Although fractionated radiation itself did not show a therapeutic effect, it seemed to sensitize tumor cells in lung cancer model mice and successfully showed a synergistic anti-tumor effect. This study has demonstrated that aerosol delivery of beclin1 enhanced the efficacy of fractionated radiotherapy. Therefore, a combination of radiation with aerosol delivery of a therapeutic gene may provide a prospect for developing novel therapy regimens applicable in clinics.

Part III

Co-delivery of LETM1 and CTMP synergistically inhibits tumor growth in H-ras12V liver cancer model mice

ABSTRACT

Since hepatocellular carcinoma (HCC) is one of the most common tumors worldwide, development of novel therapeutic approaches for HCC is urgently needed. Two different genes, LETM1 and CTMP, which target mitochondrial functions, were chosen and linked using 2A-peptide sequence. Successful self-cleavage of 2A-peptide induced synergistic anti-tumor effect in the liver of H-ras12V, the HCC model mice, by simultaneous activation of LETM1 and CTMP. Overexpression of LETM1 and CTMP significantly reduced the incidence of tumorigenesis, which were confirmed by gross and microscopic observations. Morphological changes in mitochondria, such as swelling and loss of cristae, were significant, and the prolonged activation of defects in mitochondrial function led to mitochondria-mediated apoptosis. Furthermore, with CTMP as a direct binding partner of Akt1, and LETM1 as a binding partner of CTMP, LETM1-2A-CTMP downregulated the Akt1 pathway at both Ser473 and Thr308 sites of phosphorylation. Proliferation and angiogenesis, which are important in cancer prognosis, were reduced in tumor sites after introduction of LETM1-2A-CTMP. Taken together, the results indicate that introduction of the mitochondria targeting genes, LETM1 and CTMP, and self-processing capacity of 2A-peptide sequence exerts an anti-tumor effect in liver of H-ras12V mice, suggesting its potential as a tool for gene therapy.

1. INTRODUCTION

Hepatocellular carcinoma (HCC) is the third-leading cause of death from cancer and the fifth most common malignancy worldwide (Thun *et al*., 2010). HCC is often diagnosed at an advanced stage when it is no longer susceptible to curative therapies. Highly active drug-metabolizing pathways and multidrug resistance transporter proteins in tumor cells further diminish the efficacy of current therapeutic regimens for HCC (Kota *et al*., 2009). Therefore alternative approaches are needed to overcome these barriers to enhance therapeutic efficacy.

Liver is a well-suited target organ for development of alternative strategies as it is easily targeted by both viral and non-viral gene delivery systems (Young and Dean, 2002). In this regard, non-viral gene therapy vectors based on polyethylenimine (PEI) are particularly promising. Overcoming the limitations of PEI as a gene carrier, galactosylated poly(ethylene glycol)-chitosan-graft-spermine (GPCS) copolymer was synthesized with low cytotoxicity and optimized for hepatocyte targeting using an amide bond between galactosylated poly(ethylene glycol) and chitosan-graft-spermine (Kim *et al*., 2012).

As not just one gene or protein is involved in tumorigenesis, multiple targeting is needed for an efficient therapeutic approach. Self-cleavage activity of 2A peptide has proved to be a powerful tool for simultaneous delivery of two or more genes (Fang *et al*., 2005; Szymczak and Vignali, 2005). It co-expresses functional heterologous proteins under the control of a single promoter.

Mitochondria may be the effective target of anti-cancer therapy (Decaudin *et al*., 1998;

Armstrong, 2006; Fulda *et al*., 2010). As mitochondria functions as a regulator of basic cellular functions, it has been implicated in various aspects of tumorigenesis (Gogvadze *et al*., 2008). The morphology of mitochondria has been emphasized in that it has intimate ties with cell physiology (Newmeyer and Ferguson-Miller, 2003). For example, fragmented mitochondrial morphology with disrupted cristae is correlated with apoptotic cytochrome *c* release, whereas tubular morphology promotes resistance to apoptotic stimuli (Suen *et al*., 2008). Leucine zipper/EF hand-containing transmembrane-1 (LETM1) is a mitochondrial inner membrane protein that functions in mitochondria-shaping (Dimmer *et al*., 2008). Previous study showed that LETM1 overexpression disrupts cristae of mitochondria, releases cytochrome *c* and, finally induces apoptosis in lung cancer (Hwang *et al*., 2010). Carboxyl-terminal modulator protein (CTMP) is a binding partner of Akt1 and negatively regulates its function (Maira *et al*., 2001). It has been detected in the mitochondria and a recent study determined that LETM1 is associated with CTMP to modulate mitochondrial morphology via OPA1-cleavage (Piao *et al*., 2009).

Here, linkage of LETM1 and CTMP using 2A-peptide sequence was attempted and proved its synergistic therapeutic efficacy in liver of H-ras12V, hepatocellular carcinoma model mice. Swollen mitochondria with disrupted cristae displayed increased Bax and cytochrome *c* release and induced apoptosis. These data implicate the 2A-peptide sequence as a powerful candidate to target two or more genes for therapeutic use, and both LETM1 and CTMP as putative candidates for mitochondria controlling target molecules.

2. MATERIALS AND METHODS

2.1. Materials

Antibodies against phospho-Akt1 at Thr308, phospho-Akt1 at Ser473, AMPK, Bax, cytochrome *c*, β-actin, PCNA, VEGF and FGF-2 were purchased from Santa Cruz Biotechnology (Santa Cruz, CA, USA). Monoclonal antibody against CTMP was produced using a general method described elsewhere (Hwang et al., 2007; Hwang et al., 2011; Hwang et al., 2009). Anti-Apaf-1 was obtained from Abcam (Beverly, MA, USA) and anti-LETM1 from Abnova (Taipei, Taiwan). Phospho-AMPK at Thr172 was purchased from Cell Signaling Technology (Boston, MA, USA). In Situ Cell Death Detection Kit was obtained from Roche Applied Science (Indianapolis, IN, USA). Galactosylated poly(ethylene glycol)-chitosan-*graft*-spermine (GPCS) was synthesized as previously described (Kim *et al*., 2012).

2.2. Animals

Breeding pairs of H-ras12V liver cancer model mice were obtained from Korea Research Institute of Bioscience and Biotechnology (Daejon, Korea) and maintained in a laboratory animal facility with temperature and relative humidity maintained at 23 ± 2°C and 50 ± 20%, respectively, under a 12-hour light/dark cycle. H-ras12V liver cancer model has been established as previously described (Wang *et al*., 2005), and treatment started from the age of 20 weeks when the animals starts to develop HCC.

Twenty-week-old mice were randomly divided into five groups (n=5 per group). Three expression plasmids containing LETM1, CTMP and LETM1-2A-CTMP were complexed

with GPCS and introduced to livers of the mice via tail vein injection. After eight injections (twice a week), mice were sacrificed and livers were analyzed to evaluate the therapeutic efficacy of LETM1-2A-CTMP.

2.3. Injection of GPCS / LETM1-2A-CTMP

Fifty micrograms of pLETM1-2A-CTMP were prepared in 100 ul distilled water and an appropriate amount of GPCS at a N/P ratio of 20 in same volume. By gentle vortexing, complex of GPCS with pLETM1-2A-CTMP was formed and after 30 minutes of incubation complex was injected into each H-ras12V mouse through the tail vein. After 8 times of injection within 4 weeks, mice were sacrificed and collected samples were analyzed. All experimental protocols were reviewed and approved by the Animal Care and Use Committee of Seoul National University (SNU-110628-1).

2.4. Electron microscopy

Livers were fixed in modified Karnovsky's fixative before post-fixation in 1% osmium tetroxide in 0.05 M sodium cacodylate buffer (pH 7.2). Uranyl acetate (0.5%) was used for *en bloc* staining. The livers were dehydrated in an ethanol series and embedded in Spurr's resin. Ultrathin sections were stained with 2% uranyl acetate and Reynolds' lead citrate and observed by TEM using an LIBRA 120 apparatus (Carl Zeiss, Oberkochen, Germany).

2.5. Western blot analysis

Livers were homogenized and protein concentrations were measured with a Bradford kit

(Bio-Rad, Hercules, CA, USA). An equal amount of protein (30 ug) was loaded onto an sodium dodecyl sulfate (SDS) containing gel and separated. Primary and secondary antibodies conjugated with horseradish peroxidase (Invitrogen, Carlsbad, CA, USA) were applied according to the manufacturer's protocols. Bands of interest were obtained with an LAS-3000 luminescent image analyzer (Fujifilm, Tokyo, Japan).

2.6. Histopathological examination and immunohistochemistry (IHC)

Liver sections were prepared at a thickness of 3 um on charged slide glasses (Fisher Scientific, Pittsburgh, PA, USA). Slides were stained with hematoxylin and eosin for histopathological analysis. Sections were deparaffinized, rehydrated, antigens were retrieved and endogenous peroxidase was quenched for immunohistochemistry. Primary and secondary antibodies and 3,3'-diaminobenzidine (DAB) were applied accordingly (Vector Laboratories, Burlingame, CA, USA). Slides were reviewed using a light microscope (Carl Zeiss, Thornwood, NY, USA). Staining intensity was assessed by counting the number of positive cells in randomly selected fields viewed with appropriate magnification using In Studio version 3.01 (Pixera, San Jose, CA, USA).

2.7. Terminal transferase-biotin dUTP nick end labeling (TUNEL) assay

Sections were stained by In Situ Cell Death Detection Kit after deparaffinized by xylene, ethanol and then antigens were retrieved in 0.1M citrate buffer (pH6.0). Sections were then incubated in a humidified chamber at 37°C for 1 hour with TUNEL assay mixture containing TdT enzyme (TdT enzyme mediated digoxigenin-dUTP). Slides were washed with phosphate buffered saline (PBS), incubated with Converter-AP in humidified

chamber for 30 min at room temperature and washed again. Another incubation with NBT/BCIP as a substrate for 10 min in dark, purple color was developed and examined under microscopy.

2.8. Statistical analysis

Quantification of Western blot analyses was performed with Multi-Gauge version 2.02 program (Fujifilm). All data are given as mean ± SE, and significant differences between groups were determined by unpaired *t*-test (Graphpad Software, San Diego, CA).

3. RESULTS

3.1. LETM1-2A-CTMP overexpresses both LETM1 and CTMP in vivo

LETM1 and CTMP were linked with 2A-peptide, and finally subcloned into CMV-eGFP vector (Figure III-1A). Delivery efficiency and expression of LETM1 and CTMP in livers of H-ras12V mice was evaluated by Western blot using whole lysates (Figure III-1B). As proved in previous studies (Hwang *et al*., 2007; Hwang *et al*., 2009; Hwang *et al*., 2010), LETM1 treated mice showed increase in LETM1, and CTMP treated mice showed increase in CTMP. Confirming the successful cleavage of 2A-peptide linking LETM1 and CTMP, mice treated with LETM1-2A-CTMP showed increase in both LETM1 and CTMP (Figure III-1C and 1D).

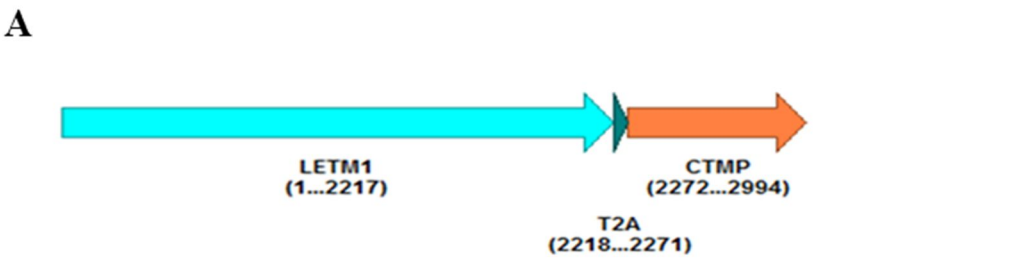
A
LETM1
(1...2217)
CTMP
(2272...2994)
T2A
(2218...2271)

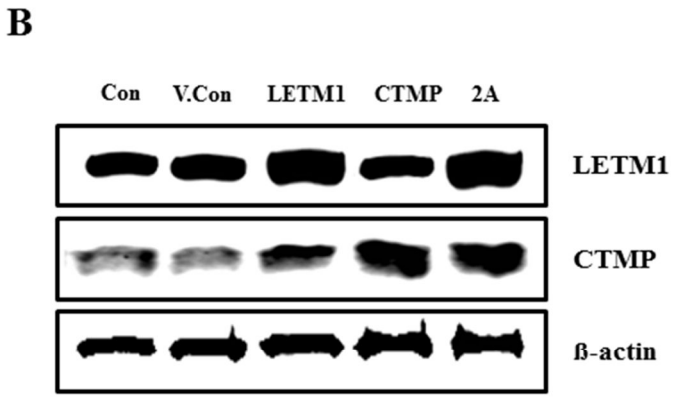
B
Con
V.Con
LETM1
CTMP
2A
LETM1
CTMP
ß-actin

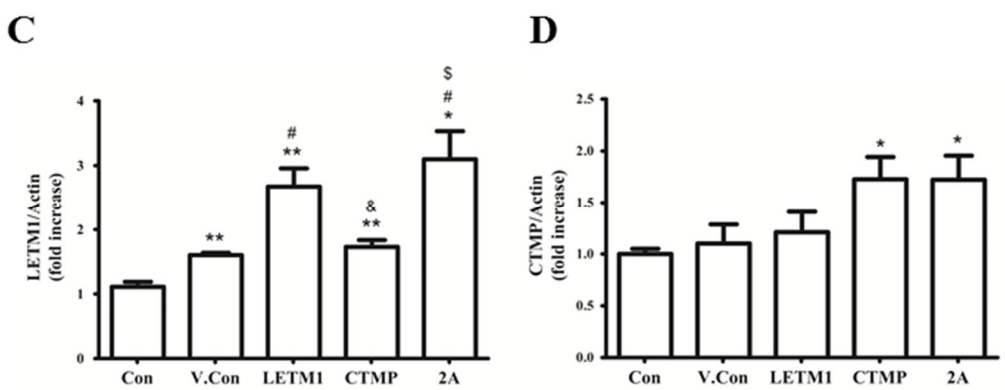
C
LETM1/Actin
(fold increase)
Con
V.Con
LETM1
CTMP
2A
D
CTMP/Actin
(fold increase)
Con
V.Con
LETM1
CTMP
2A

Figure III-1. Delivery of GPCS/LETM1-2A-CTMP to livers of H-ras12V mice. A. Cloning scheme of LETM1-2A-CTMP. LETM1 (2217 bp) and CTMP (718 bp) have been linked using 2A-peptide cleavage sequence. **B.** Protein levels of LETM1 and CTMP were determined by Western blot using total lysates. Successful cleavage has been confirmed by overexpressed protein level of both LETM1 and CTMP in LETM1-2A-CTMP group. Bands are representative of five individuals from each group. **C.** Densitometric analysis of Western blot. Each bar represents the mean±S.E (n=5). * $p<0.1$ compared to control, ** $p<0.01$ compared to control, # $p<0.05$ compared to vector control, & $p<0.05$ compared to LETM1, $ $p<0.05$ compared to CTMP.

3.2. LEMT1-2A-CTMP significantly slows progression of liver cancer in H-ras12V mice

In gross morphology, 24-week-old H-ras12V mice showed various-sized tumors on the surface of the liver. When therapeutic genes were introduced to the animals, both the size and number of tumor nodules were markedly reduced (Figure III-2, upper panel). Decrease in tumor size was confirmed after hematoxylin and eosin staining of the tissue section (Figure III-2, middle panel). Under higher magnification, focusing on the cell morphology at the margin of normal and tumor tissue, cells transformed into longitudinal shape were evident (Figure III-2, bottom panel) and mitotic figures were present in tumor lesions of non-treated groups (Figure III-2, upper right corner of bottom panel). Histopathologically, lesions were graded into altered foci (well-demarcated foci with minimal cytological changes), hepatocellular adenomas (benign neoplasmic lesions where hepatocytes proliferate with numerous thin-walled vessels, without portal tracts) and hepatocellular adenocarcinomas (malignant neoplasmic lesions with well differentiated larger hepatocytes, frequently with polymorphic nucleus and mitotic figures). In non-treated groups, control and vector control, malignant signs of hepatocellular adenocarcinoma, such as mitotic figures, were shown. CTMP, LETM1 and LETM1-2A-CTMP treated mice remained in benign state, with hepatocellular adenoma and altered foci (Table III).

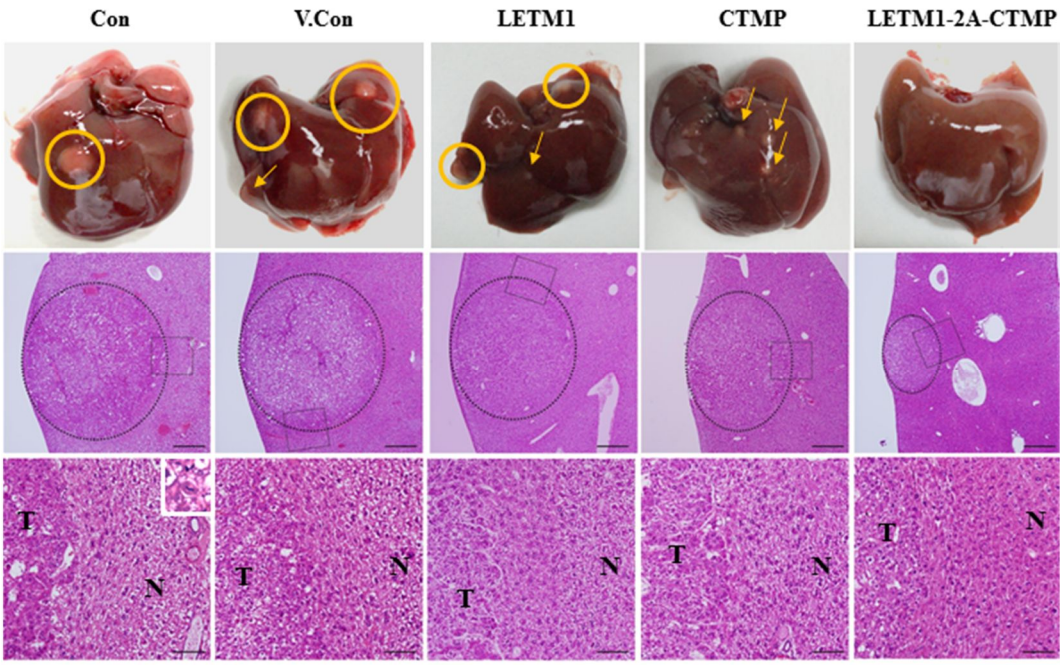

Figure III-2. Gross morphology and histopathological analysis of tumors in livers of H-ras12V mice. (Upper) Representative pictures of the livers. Circles indicate tumor size >2.5mm. Arrows indicate tumor size <2.5mm. (Middle) Lesions of livers; hematoxylin and eosin stained. Scale bar ; 20 um. Dotted circles indicate tumor nodules and boxed parts were magnified in lower panel. Mitotic figure, representative feature of hepatocellular carcinoma, is presented on right corner of lower Control panel. Scale bar ; 50 um. T; tumor, N; normal.

Table III. Summary of tumor incidence in the livers of H-ras12V mice

Group	Number of Mice	Number of Tumors/ mouse			Adenocarcinoma	Adenoma [a]		
		Total	>1mm	<1mm		+++	++	+
Con	7	15.11±1.96	7.55±1.66	7.55±2.29	5	2	0	0
V.Con	7	13.89±3.60	5.94±1.70	8.11±3.15	6	0	1	0
BECN1	7	5.55±2.40***	2.50±1.69***	2.88±1.53***	2	0	4	1

Twenty-five H-ras12V liver cancer model mice were randomly divided into 5 groups ; Control, Vector Control, LETM1, CTMP and LETM1-2A-CTMP. Animals were put into experiment by the age of 20 weeks, when H-ras12V model starts to develop hepatocellular carcinoma (HCC). After 8 times of treatment in 4 weeks, animals were sacrificed and livers were collected for histopathological analysis. Livers from five mice were fixed in 10% neutral buffered formalin for histological examination. Progression of carcinogenesis in livers were graded into 3 categories ; hepatocellular carcinoma (HCC), hepatocellular adenoma (HCA), altered foci.

3.3. LETM1-2A-CTMP showed anti-tumor effect via mitochondria-mediated apoptosis

LETM1 is located in inner mitochondrial membrane. As previously reported, a role of CTMP in mitochondrial-mediated apoptosis (Hwang *et al.*, 2010). Appropriately, the morphology of mitochondria was presently observed using transmission electron microscopy (TEM). Introduction of LETM1 and CTMP induced swelling of mitochondria and disruption of cristae, but the morphology of nucleus remained intact. However, proving that LETM1-2A-CTMP synergistically induces more cell death in tumors, nuclei in LETM1-2A-CTMP treated mice began to show apoptotic signs. Nuclear fragmentation, condensed chromatin lining and indentations of the nuclear membrane were observed with mitochondria defects (Figure III-3A). Apaf-1, Bax and cytochrome *c* were screened as representatives of mitochondria-mediated apoptosis by Western blot. These apoptosis-related proteins were increased following treatment with LETM1 and CTMP. LETM1-2A-CTMP further induced mitochondria-mediated apoptosis and a significant increase in apoptosis-related proteins was observed (Figure III-3B and 3C). TUNEL assay indicated significant apoptotic cells with treatment using LEMT1 and CTMP, and still more in LETM1-2A-CTMP treatment (Figure III-3D). TUNEL-positive cells were counted at five different fields of each slide and statistical analysis confirmed the results with high significance (Figure III-3E).

A

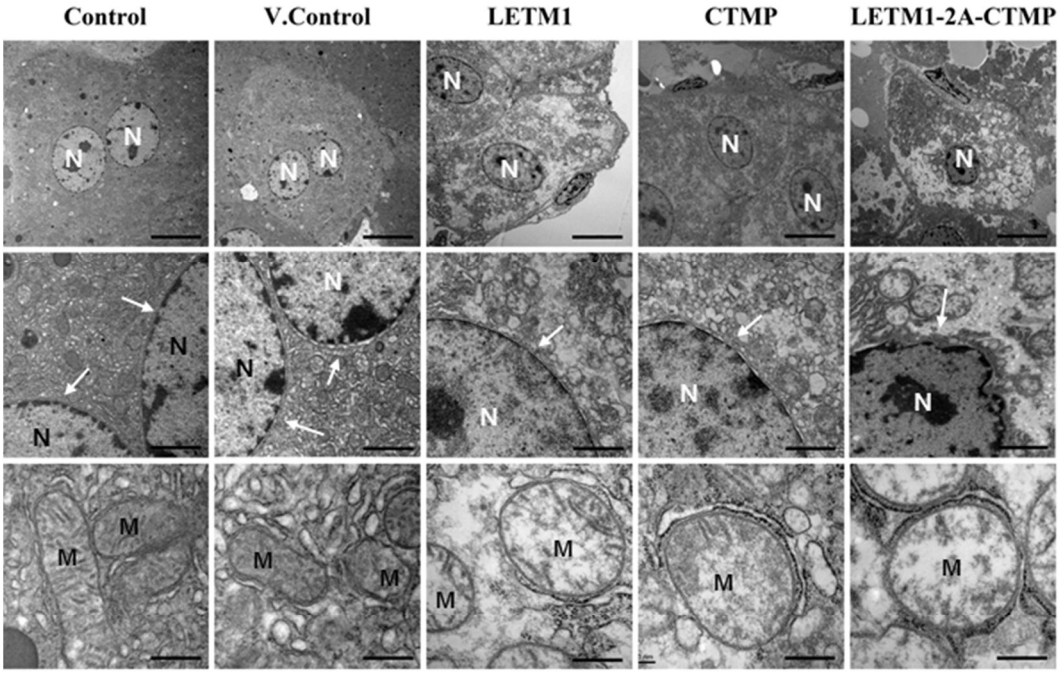
Control
V.Control
LETM1
CTMP
LETM1-2A-CTMP
N
M

B

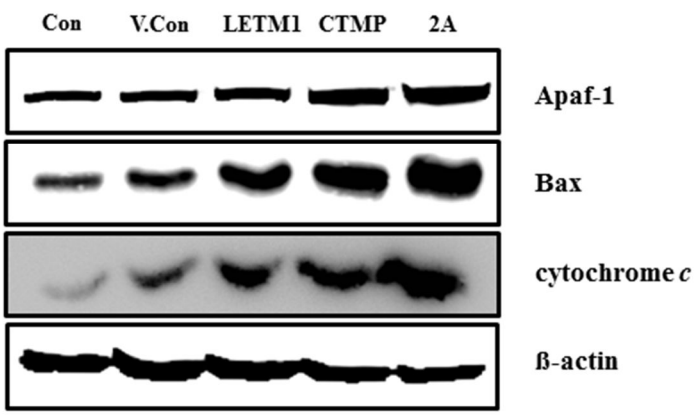
Con
V.Con
LETM1
CTMP
2A
Apaf-1
Bax
cytochrome c
ß-actin

C

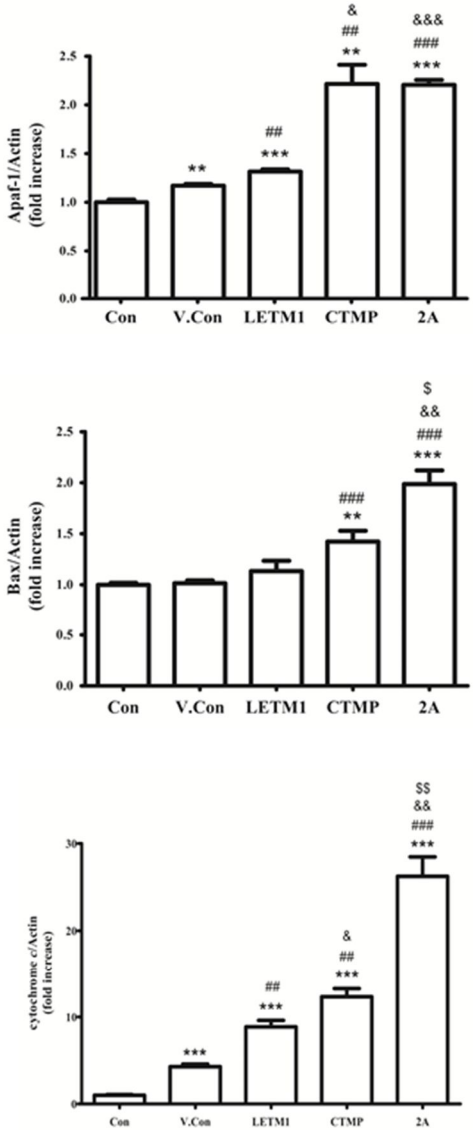
Apaf-1/Actin
(fold increase)
2.5
2.0
1.5
1.0
0.5
0.0
**
##
***
&
##
**
&&&
###
***
Con
V.Con
LETM1
CTMP
2A
Bax/Actin
(fold increase)
2.5
2.0
1.5
1.0
0.5
0.0
###
**
$
&&
###
***
Con
V.Con
LETM1
CTMP
2A
cytochrome c/Actin
(fold increase)
30
20
10
0
***
##
***
&
##
***
$$
&&
###
***
Con
V.Con
LETM1
CTMP
2A

D

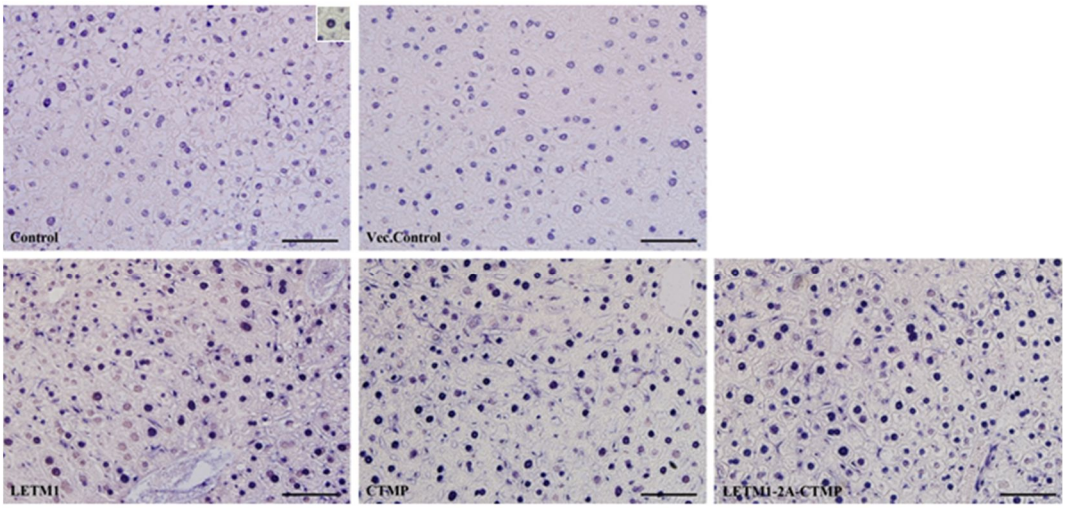
Control
Vec.Control
LETM1
CTMP
LETM1-2A-CTMP

E

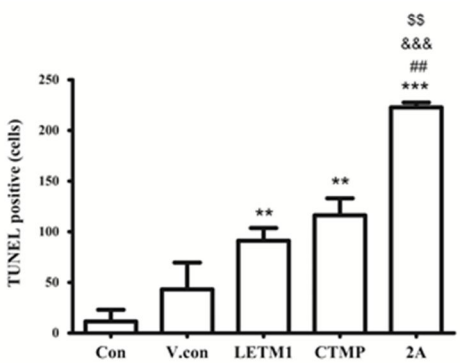
$$
&&&
##
***
**
**
TUNEL positive (cells)
250
200
150
100
50
0
Con
V.con
LETM1
CTMP
2A

F

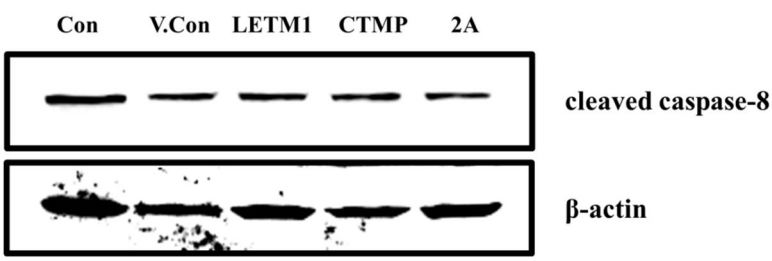
Con
V.Con
LETM1
CTMP
2A
cleaved caspase-8
β-actin

Figure III-3. Mitochondria related apoptosis in livers of H-ras12V mice. A. Transmission electron microscopy of tumors. (Upper) Morphology of whole hepatocyte. Scale bar ; 5 um. (Middle) Morphology of nucleus. Arrows indicate nuclear membrane. Scale bar ; 1 um. (Lower) Morphology of mitochondria. Scale bar ; 200nm. N; nucleus, M; mitochondria. **B.** Protein levels of Apaf-1, Bax and cytochrome *c* were determined by Western blot using total lysates. **C.** Densitometric analysis of Western blot (n=5/group). Each bar represents the mean±S.E (n=5). ** $p<0.01$ compared to control, *** $p<0.005$ compared to control, ## $p<0.01$ compared to vector control, ### $p<0.005$ compared to vector control, & $p<0.05$ compared to LETM1, && $p<0.01$ compared to LETM1, &&& $p<0.005$ compared to LETM1, $ $p<0.05$ compared to CTMP, $$ $p<0.01$ compared to CTMP. **D.** TUNEL assay on tumor region. TUNEL positive cells presented on upper right corner of control panel. Scale bar : 20 um. **E.** TUNEL positive cells were counted and graphed. Each bar represents the mean±S.E (n=5). ** $p<0.01$ compared to control, *** $p<0.005$ compared to control, ## $p<0.01$ compared to vector control, &&& $p<0.005$ compared to LETM1, $$ $p<0.01$ compared to CTMP. **F.** Protein levels of cleaved caspase-8 was determined by Western blot using total lysates. Changes were noted minor, adding to the finding that mitochondria-dependent apoptosis was activated in LETM1-2A-CTMP induced mice.

3.4. LETM1-2A-CTMP produces anti-tumor effect via downregulation of Akt1

CTMP was initially identified as a cytosolic interactor of Akt1. Western blot analyses were performed to examine the levels of CTMP, as a binding partner of Akt1, and AMPK, as a negative regulator of Akt1. The total AMPK level remained the same even after the introduction of LETM1, CTMP and LETM1-2A-CTMP. However, phosphorylated AMPK at Thr172 showed a very significant increase in LETM1 and LETM1-2A-CTMP (Figure III-4A and 4B). Total Akt1 did not change, but phosphorylation of Akt1 at Ser473 and Thr308 decreased accordingly (Figure III-4C). After statistical analysis, the effect of LETM1-2A-CTMP in Akt1 phosphorylation proved to be significant (Figure III-4D).

A

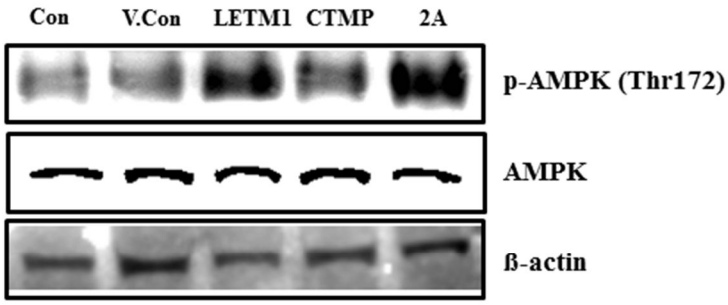
Con
V.Con
LETM1
CTMP
2A
p-AMPK (Thr172)
AMPK
ß-actin

B

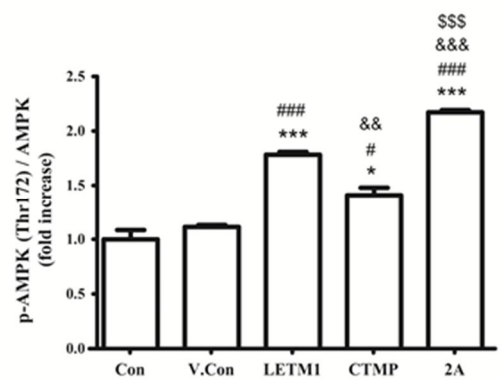
p-AMPK (Thr172) / AMPK
(fold increase)
2.5
2.0
1.5
1.0
0.5
0.0
###
***
&&
#
*
$$$
&&&
###
***
Con
V.Con
LETM1
CTMP
2A

C

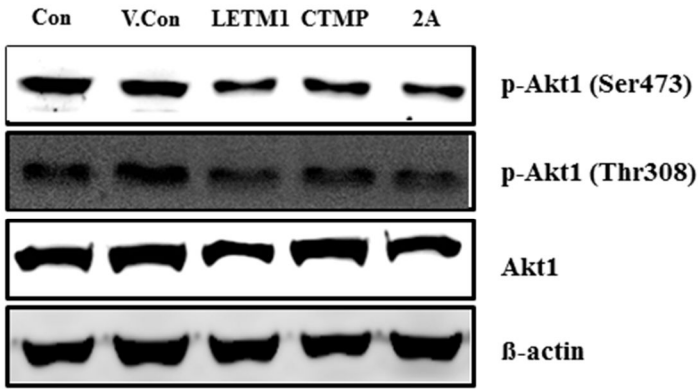
Con
V.Con
LETM1
CTMP
2A
p-Akt1 (Ser473)
p-Akt1 (Thr308)
Akt1
ß-actin

D

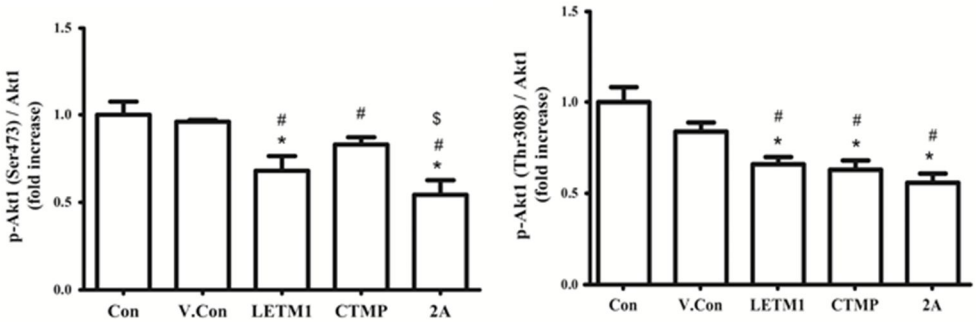
p-Akt1 (Ser473) / Akt1
(fold increase)
1.5
1.0
0.5
0.0
Con
V.Con
LETM1
CTMP
2A
p-Akt1 (Thr308) / Akt1
(fold increase)

Figure III-4. Synergistic anti-tumor effect via AMPK-AKT pathway in livers of H-ras12V mice. A. Protein levels of p-AMPK(Thr172) and AMPK were determined by Western blot using total lysates. **B.** Densitometric analysis of Western blot. Each bar represents the mean±S.E (n=5). * $p<0.05$ compared to control, *** $p<0.005$ compared to control, ### $p<0.005$ compared to vector control, && $p<0.01$ compared to LETM1, &&& $p<0.005$ compared to LETM1, $$$ $p<0.005$ compared to CTMP. **C.** Protein levels of p- Akt1 (Ser473), p- Akt1 (Thr308) and Akt1 were determined by Western blot using total lysates. **D.** Densitometric anlaysis of Western blot. Each bar represents the mean±S.E (n=5). * $p<0.05$ compared to control, # $p<0.05$ compared to vector control, $ $p<0.05$ compared to CTMP.

3.5. LETM1-2A-CTMP reduces cell proliferation in H-ras12V liver cancer model mice

Proliferating cell nuclear antigen (PCNA) is expressed in the nuclei of cells during DNA synthesis phase of the cell cycle. To investigate the capacity of cancer cell proliferation, PCNA protein level was determined with Western blot using whole lysate. LETM1-2A-CTMP produced significant inhibition of proliferation compared to LETM1 or CTMP alone (Figure III-5A and 5B). The level of PCNA protein was further examined with immunohistochemistry; a decreasing pattern of PCNA positive cells was detected. PCNA positive cells were counted at five different fields of each slide and statistical analysis confirmed the significant synergistic anti-tumor effect (Figure III-5C and 5D).

A

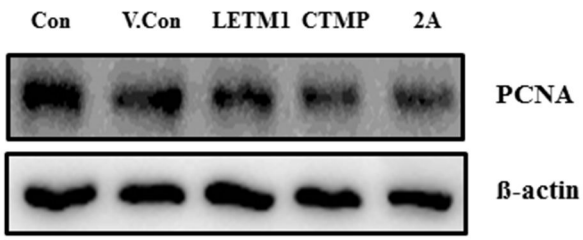
Con
V.Con
LETM1
CTMP
2A
PCNA
ß-actin

B

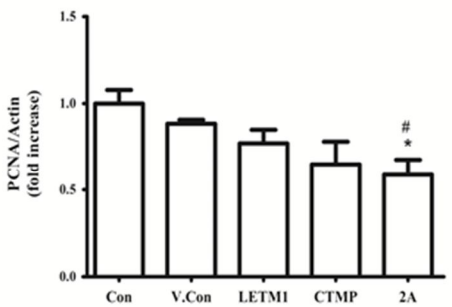
PCNA/Actin
(fold increase)
1.5
1.0
0.5
0.0
#
*
Con
V.Con
LETM1
CTMP
2A

C

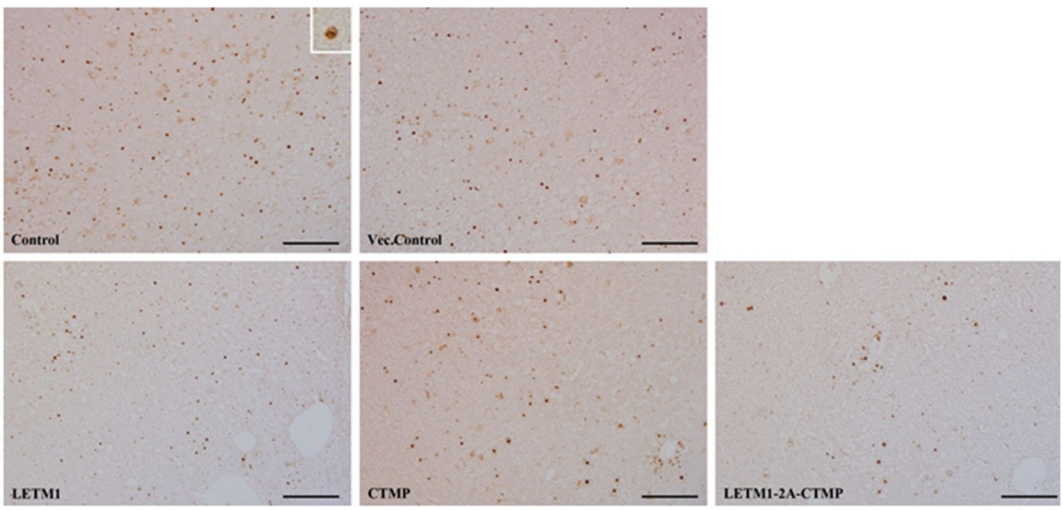
Control
Vec.Control
LETM1
CTMP
LETM1-2A-CTMP

D

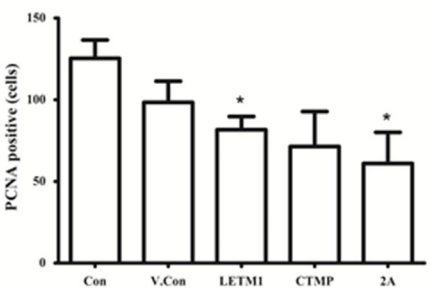
PCNA positive (cells)
150
100
50
0
*
*
Con
V.Con
LETM1
CTMP
2A

Figure III-5. Analysis of proliferation in livers of H-ras12V mice. A. Protein level of PCNA was determined by Western blot using total lysates. **B.** Densitometric analysis of Western blot. Each bar represents the mean±S.E (n=5). *p <0.05 compared to control, #p<0.05 compared to vector control. **C.** Immunohistochemistry of PCNA on margin of tumor and normal region. PCNA positive cells presented on upper right corner of control panel. **D.** PCNA positive cells were counted and graphed (n=5/group). * p <0.05 compared to control.

3.6. LEMT1-2A-CTMP reduces angiogenesis in H-ras12V liver cancer model mice

Neovasculization is one of the main characteristics of tumorigenesis. Vascular endothelial growth factor (VEGF) is a signal protein produced by cells. VEGF stimulates vasculogenesis and angiogenesis. VEGF of LETM1-2A-CTMP was significantly decreased compared to control and vector control. Fibroblast growth factor-2 (FGF-2) is present in the subendothelial extracellular matrix of blood vessels and is activated in tumor development. FGF-2, as a potent angiogenic growth factor, was decreased significantly in LETM1-2A-CTMP treated mice (Figure III-6A and 6B). Immunohistopathological staining confirmed the decreasing VEGF (Figure III-6C) and FGF-2 (Figure III-6D) in margins of normal to tumor areas of each group.

A

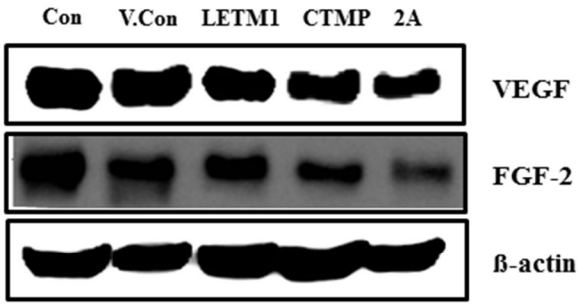
Con
V.Con
LETM1
CTMP
2A
VEGF
FGF-2
ß-actin

B

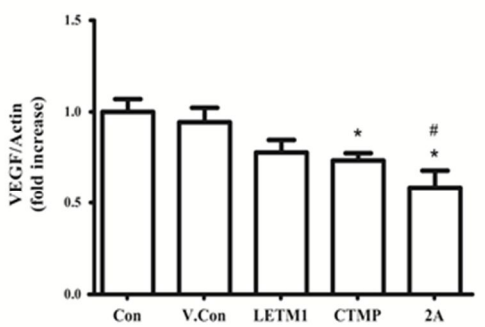
VEGF/Actin
(fold increase)
1.5
1.0
0.5
0.0
*
#
*
Con
V.Con
LETM1
CTMP
2A

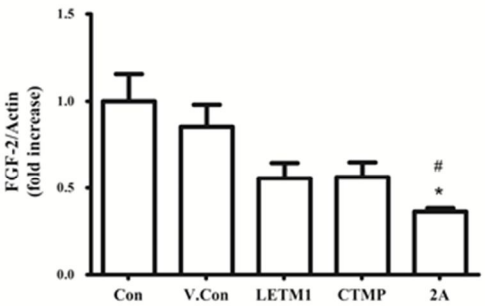
FGF-2/Actin
(fold increase)
1.5
1.0
0.5
0.0
#
*
Con
V.Con
LETM1
CTMP
2A

C

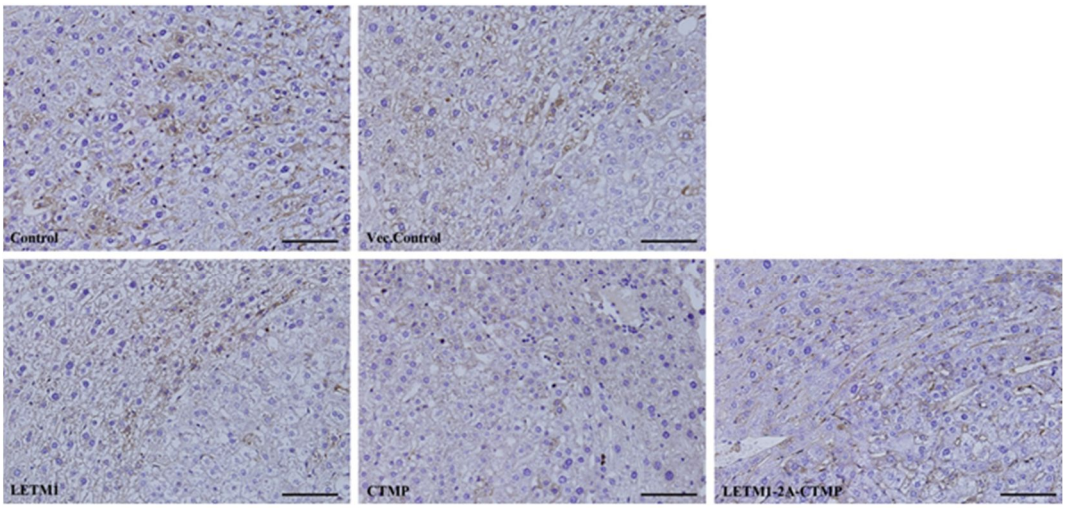
Control
Vec.Control
LETM1
CTMP
LETM1-2A-CTMP

D

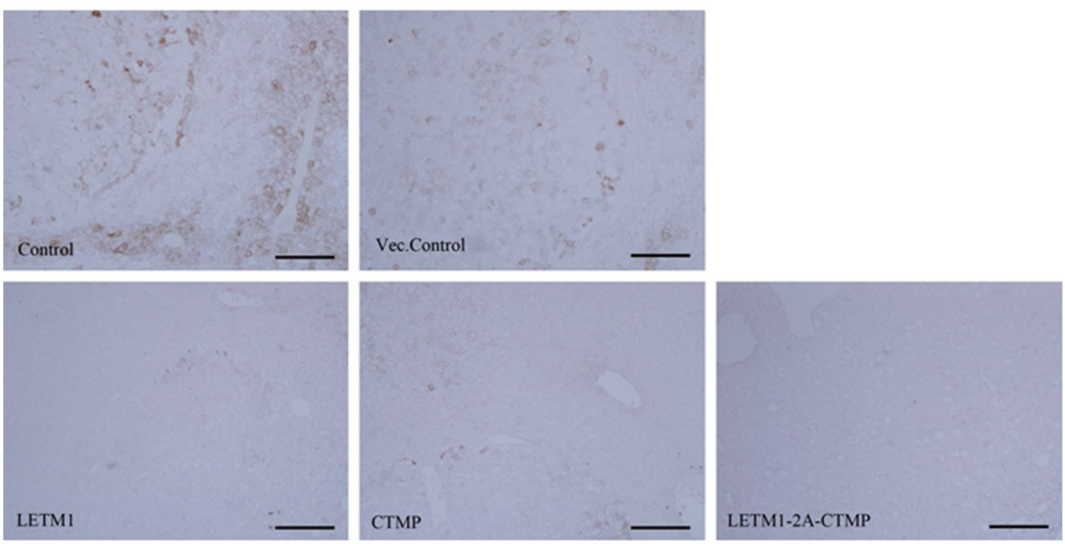
Control
Vec.Control
LETM1
CTMP
LETM1-2A-CTMP

Figure III-6. Analysis of angiogenesis in livers of H-ras12V mice. **A**. Protein levels of VEGF, FGF-2 were determined by Western blot using total lysates. **B**. Densitometric analysis of Western blot. Each bar represents the mean±S.E (n=5). * $p < 0.05$ compared to Control, # $p<0.05$ compared to vector control. $ $p<0.05$ compared to CTMP. **C**. Immunohistochemistry of VEGF counterstained with hematoxylin, margin of tumor and normal region. **D**. Immunohistochemistry of FGF-2 counterstained with hematoxylin, margin of tumor and normal region.

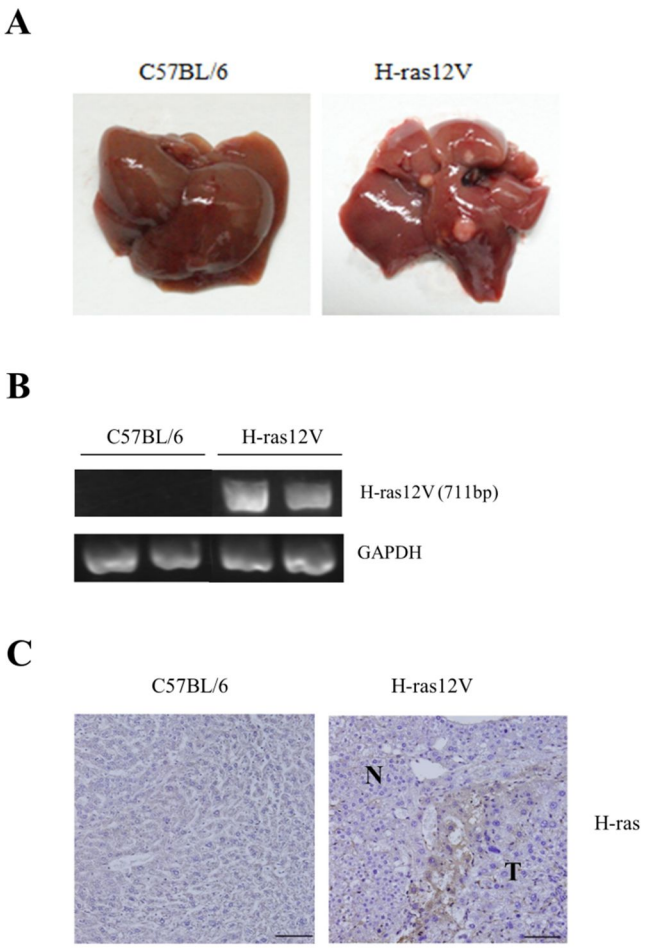

Figure III-7. Confirmation of H-ras12V used in the experiment. A. Gross morphology of livers at the age of 20 weeks. Tumor nodules on the surface are remarkable in H-ras12V, hepatocellular carcinoma (HCC) model. B. Genomic DNA was extracted from tails of each individual and polymerase chain reaction (PCR) was performed to see H-ras12V expression. Primer sequences for H-ras12V PCR are F ; 5'-CTAGGGCT GCAGGAATTC-3', R ; 5'-GTAGTTTAACACATTATACACT-3'. C. Immunohisto-chemistry of H-ras in the margin of normal and tumor tissue. N ; Normal, T ; Tumor.

4. DISCUSSION

The use of self-cleavage 2A peptide sequence to express multiple proteins with single promoter is a promising area in biology research (Szymczak and Vignali, 2005). However, the use of 2A peptide has been limited to the field of generating transgenic animals, especially pigs, in that it makes possible to express multiple proteins through a single round of nuclear transfer (Trichas *et al*., 2008; Deng *et al*., 2011). Here, exploration on the self-cleavage potential of 2A peptide sequence to target two different genes, LETM1 and CTMP, was attempted in treatment of hepatocellular carcinoma (HCC). Even though ras activation is not common in human HCC, activated mutations in ras have been found in all human tumors, and the frequency of ras mutations was the highest among the genes that are associated with cancers (Hunter, 1997). Murine HCCs also express H-ras, which is activated in 70% of cases, supporting the view that H-ras plays a key role in hepatocarcinogenesis.

Use of two independent transcriptional units to express two different genes may create an imbalance of expression levels according to the order inside the expression vector (Xu *et al*., 1989; McLachlin *et al*., 1993). However, when designing an expression vector using the 2A peptide sequence, the order of the target genes does not need to be taken into consideration. As it shares single promoter and cleavage occurs at the end of 2A peptide, the genes should be expressed in independent manners once cleaved successfully (Szymczak and Vignali, 2005).

Delivery and cleavage efficiency of 2A peptide was confirmed with Western blot (Figure III-1B) and following statistical analysis (Figure III-1C). The lack of a shift in

protein size for both LETM1 and CTMP in liver homogenates of H-ras12V mice, treated with LETM1, CTMP and LETM1-2A-CTMP, provided the evidence that the cleavage of 2A peptide was successful (data not shown). The extent of overexpression varied, however, in that LETM1 was prominently evident compared to CTMP. This may not due to the efficiency of 2A peptide, but may reflect the nature of target gene expression itself, as mice treated only with LETM1 or CTMP showed the same pattern of each gene, as compared to mice treated with LETM1-2A-CTMP.

H-ras12V model starts to develop hepatocellular carcinoma (HCC) from the age of 20 weeks. In H-ras12V mice, tumor nodules can be observed on the surface of the livers, H-ras12V gene can be detected in genomic DNA and H-ras protein expresses in the margin of normal and tumor region (Figure III-7). Efficacy evaluation of 2A peptide in livers of H-ras12V, HCC model mice revealed the decrease of the prominent nodules on the surface of the organ (Figure III-2). Histopathological analysis confirmed that introduction of therapeutic genes (LETM1, CTMP and LETM1-2A-CTMP) slowed down the progression of altered foci to hepatocellular adenocarcinoma (Table III). LETM1 and CTMP alone have shown therapeutic effects in lungs of K-ras^{LA1}, lung cancer model mice in previous studies (Hwang *et al.,* 2007; Hwang *et al.,* 2009; Hwang *et al.,* 2010). Also, the present data gained from the HCC model support the possibility of LETM1 and CTMP as the therapeutic candidates.

The mitochondrion is a central component of cellular maintenance and many studies have been focused on exploring its mechanisms related to diseases directly related to energy metabolism, such as Parkinson's disease (Gu *et al.,* 1998; Schapira *et al.,* 1990) and various cancers (Carew and Huang, 2002; Brandon *et al.,* 2006; Chatterjee *et al.,*

2006; Gogvadze *et al.,* 2008). As both LETM1 and CTMP have been reported to participate in maintaining the morphology of mitochondria (Dimmer *et al.,* 2008; Parcellier *et al.,* 2009), overexpression of both was expected to bring mitochondrial defects capable of inducing cancer cell death. Under normal progress towards HCC, mitochondria should show a tubular morphology, which promotes resistance to apoptotic stimuli (Suen *et al.,* 2008). (Figure III-3A, control and vector control panels) However, under stress of LETM1 and CTMP overexpression, swollen and fragmented mitochondrial morphology with disrupted cristae were observed (Figure III-3A, LETM1 and LETM1-2A-CTMP panels). Interestingly, disruption of the nuclear membrane with indication of apoptosis was only detectable in LETM1-2A-CTMP treated mice (Figure III-3A, middle panel), which was further investigated with Western blot analysis. Mitochondrial disruption in the presence of LETM1 and CTMP, and nuclear disruption in the presence of LETM1-2A-CTMP correlated with increases in Bax and Apaf-1, and the release of apoptotic cytochrome *c* (Figure III-3B). Bax is a proapoptotic protein that induces cell death by acting on mitochondria (Wolter *et al.,* 1997; Marzo *et al.,* 1998). Cytochrome *c* binding to Apaf-1, triggers caspase-3 dependent apoptosis pathway activation (Li *et al.,* 1997; Perkins *et al.,* 2000), also increased in accordance with the TEM-evident morphology of disrupted mitochondria. Changes in cleaved caspase-8 was minor, confirming the phenomenon of mitochondria-dependent apoptosis is prominent (Figure III-3F). When cross-confirmed with TUNEL assay for DNA fragmentation, TUNEL positive cells were increased significantly in the LETM1-2A-CTMP treated group (Figure III-3C and 3D).

When cells are under stress of growth and biosynthetic synthesis suppression, such as

exposure of cancer cells to therapeutic agents, AMP kinase (AMPK) is activated accordingly (Gwinn *et al.,* 2008). In this study, introduction of LETM1, CTMP and LETM1-2A-CTMP phosphorylated AMPK at Thr172, leading to the activation of the energy sensor AMPK (Figure III-4A and 4B). Interestingly, mice treated solely with CTMP showed lesser increase in AMPK phosphorylation due to the indirect connection with mitochondria and phosphoinositol-3-kinase (PI3K)-Akt. One report described that activation of AMPK in HCC is capable of suppressing cancer cell growth (Ziang *et al.,* 2004), which supports the present idea that activation of AMPK phosphorylation induced HCC regression. Constitutive activation of PI3K-Akt signaling has been reported in many cancers including glioblastoma, advanced prostate cancer (Motoshima *et al.,* 2006) and HCC (Fleischer *et al.,* 2006). Phosphorylation of Akt1 both at Ser473 and Thr308 decreased when exposed to LETM1, CTMP and LETM1-2A-CTMP (Figure III-4C and 4D), satisfying the notion that LETM1, CTMP and LETM1-2A-CTMP led to mitochondrial disruption followed by apoptosis by suppressing the Akt1 pathway.

Important factors to consider in evaluating the therapeutic efficacy of tumorigenesis are the proliferative and angiogenic capabilities of tumor cells. PCNA has been reported as a highly sensitive marker for cell proliferation (Miller *et al.,* 1999). Total homogenates of livers showed decrease in PCNA. Also, from the tumor sites, proliferating cells were significantly reduced with the well-demarcated fibrotic margin (Figure III-5A and 5B). VEGF is a potent endothelial cell mitogen and key regulator of both physiologic and pathologic angiogenesis (Wong *et al.,* 2001; Niu *et al.,* 2002). FGF-2 is an important stimulator of angiogenesis that has been implicated in neoplastic progression and which is a potent mitogen for different cell types, including vascular endothelial cells and

fibroblasts (Seghezzi *et al.,* 1998). Attempts to neutralize or modulate FGF-2 have met with some success in controlling neovascularity and tumor growth (Plum *et al.,* 2000). As both VEGF and FGF-2 were decreased in mice treated with LETM1, CTMP and LETM1-2A-CTMP, with the decrease being more pronounced for the 2A peptide form, the synergistic effect of dual gene targeting with 2A peptide is confirmed (Figure III-6).

In summary, the results clearly demonstrate the dual targeting of LETM1 and CTMP using 2A peptides in H-ras12V, HCC model mice. Successful cleavage of 2A peptide sequence induced a synergistic anti-tumor effect by disrupting mitochondria morphology and leading to mitochondria-mediated apoptosis via activation of the AMPK and Akt1 pathways. Furthermore, proliferative and angiogenic capability of tumor cells decreased as a final output of the therapeutic effects. Here the overall data ultimately suggest that application of 2A peptide sequence *in vivo* to target two or more genes and selection of multiple genes targeting mitochondria for cancer therapy are promising approaches toward development of cancer therapeutics.

REFERENCE

Adams GE, Ahmed I, Sheldon PW, Stratford IJ. Radiation sensitization and chemopotentiation: RSU 1069, a compound more efficient than misonidazole in vitro and in vivo. *Br J Cancer* 1984; 49(5): 571-577.

Albert JM, Cao C, Kim KW, Willey CD, Geng L, Xiao D, Wang H, Sandler A, Johnson DH, Colevas AD, Low J, Rothenberg ML, Lu B. Inhibition of poly (ADP-ribose) polymerase enhances cell death and improves tumor growth delay in irradiated lung cancer models. *Clin Cancer Res* 2007; 13(10): 3033-3042.

Alexandridou S, Kiparissides C, Mange F, Foissy A. Surface characterization of oil-containing polyterephthalamide microcapsules prepared by interfacial polymerization. *J Microencapsul* 2001; 18(6): 767-781.

Alton EW, Middleton PG, Caplen NJ, Smith SN, Steel DM, Monkonge FM, Jeffery PK, Geddes DM, Hart SL, Williamson R, Fasold KI, Miller AD, Dickinson P, Stevenson BJ, MacLachlan G, Dorin JR, Porteous DJ. Non-invasive liposome-mediated gene delivery can correct the ion transport defect in cystic fibrosis mutant mice. *Nat Genet* 1993; 5(2): 135-142.

Armstrong JS. Mitochondria : a target for cancer therapy. *Br J Pharmacol* 2006; 147(3): 239-248

Arote R, Kim TH, Kim YK, Hwang SK, Jiang HL, Song HH, Nah JW, Cho MH, Cho CS.

A biodegradable poly (ester amine) based on polycaprolactone and polyethylenimine as a gene carrier. *Biomaterials* 2007; 28(4): 735-744.

Azad MB, Chen Y, Henson ES, Cizeau J, McMillan-Ward E, Israels SJ, Gibson SB. Hypoxia induces autophagic cell death in apoptosis-competent cells through a mechanism involving BNIP3. *Autophagy* 2008; 4(2): 195-204.

Brady LW, Heilmann HP, Molls M. Advances in Radiation Oncology in Lung Cancer. Berlin: Springer-Verlag; 2005.

Brandon M, Baldi P, Wallace D. Mitochondrial mutations in cancer. *Oncogene* 2006;25: 4647-4662.

Brech A, Ahlquist T, Lothe RA, Stenmark H. Autophagy in tumour suppression and promotion. *Mol Oncol* 2009; 3(4): 366-375.

Carew JS, Huang P. Mitochondrial defects in cancer. *Mol Cancer* 2002;1: 9.

Chatterjee A, Mambo E, Sidransky D. Mitochondrial DNA mutations in human cancer. *Oncogene* 2006; 25(34): 4663-4674.

Chen N, Karantza V. Autophagy as a therapeutic target in cancer. *Cancer Biol Ther* 2011;11(2): 157-168.

Chen R, Kim O, Yang J, Sato K, Eisenmann KM, McCarthy J, Chen H, Qiu Y. Regulation of Akt/PKB activation by tyrosine phosphorylation. *J Biol Chem* 2001; 276(34): 31858-31862.

Choe G, Horvath S, Cloughesy TF, Crosby K, Seligson D, Palotie A, Inge L, Smith BL, Sawyers CL, Mischel PS. Analysis of the phosphatidylinositol 3′-kinase signaling pathway in glioblastoma patients in vivo. *Cancer Res* 2003; 63(11): 2742-2746.

Ciechomska IA, Goemans GC, Skepper JN, Tolkovsky AM. Bcl-2 complexed with beclin-1 maintains full anti-apoptotic function. *Oncogene* 2009; 28(21): 2128-2141.

Dachs GU, Dougherty GJ, Stratford IJ, Chaplin DJ. Targeting gene therapy to cancer: a review. *Oncol Res* 1997; 9(6-7): 313-325.

De Pol A, Vaccina F, Forabosco A, Cavazzuti E, Marzona L. Apoptsis of gern cells during human prnatal oogenesis. *Hum Reprod* 1997; 12(10): 2235-2241.

Debnath J, Baehrecke EH, Kroemer G. Does autophagy contibute to cell death? *Autophagy* 2005; 1(2): 66-74.

Decaudin D, Marzo I, Brenner C, Kroemer G. Mitochondria in chemotherapy-induced apoptosis: a prospective novel target of cancer therapy (review). *Int J Oncol* 1998; 12(1): 141-152.

Deng W, Yang D, Zhao B, Ouyang Z, Song J, Fan N, Liu Z, Zhao Y, Wu Q, Nashun B, Tang J, Wu Z, Gu W, Lai L. Use of the 2A peptide for generation of multi-transgenic pigs through a single round of nuclear transfer. *PLoS One* 2011; 6(5): e19986.

Dimmer KS, Navoni F, Casarin A, Trevisson E, Endele S, Winterpacht A, Salviati L, Scorrano L. LETM1, deleted in Wolf–Hirschhorn syndrome is required for normal

mitochondrial morphology and cellular viability. *Hum Mol Genet* 2008; 17(2): 201-214.

Dorin JR, Farley R, Webb S, Smith SN, Farini E, Delaney SJ, Wainwright BJ, Alton EW, Porteous DJ. A demonstration using mouse models that successful gene therapy for cystic fibrosis requires only partial gene correction. *Gene Ther* 1996; 3(9): 797-801.

Dvorak HF. Vascular permeability factor/vascular endothelial growth factor: a critical cytokine in tumor angiogenesis and a potential target for diagnosis and therapy. *J Clin Oncol* 2002; 20(21): 4368-4380.

Edinger AL, Thompson CB. Death by design: apoptosis, necrosis and autophagy. *Curr Opin Cell Biol* 2004;16(6): 663-669.

Elmore S. Apoptosis: a review of programmed cell death. *Toxicol Pathol* 1007; 35(4): 495-516.

Fang J, Qian JJ, Yi S, Harding TC, Tu GH, VanRoey M, Jooss K. Stable antibody expression at therapeutic levels using the 2A peptide. *Nat Biotechnol* 2005; 23(5): 584-590.

Ferrara N. Vascular endothelial growth factor: basic science and clinical progress. *Endocr Rev* 2004; 25(4): 581-611.

Fleischer B, Schulze-Bergkamen H, Schuchmann M, Weber A, Biesterfeld S, Müller M, Krammer PH, Galle PR. Mcl-1 is an anti-apoptotic factor for human hepatocellular

carcinoma. *Int J Oncol* 2006; 28(1): 25-32.

Fujita N, Sato S, Katayama K, Tsuruo T. Akt-dependent phosphorylation of p27Kip1 promotes binding to 14-3-3 and cytoplasmic localization. *J Biol Chem* 2002; 277(32): 28706-28713.

Fulda S, Galluzzi L, Kroemer G. Targeting mitochondria for cancer therapy. *Nat Rev Drug Discov* 2010; 9(6): 447-464.

Furler S, Paterna JC, Weibel M, Büeler H. Recombinant AAV vectors containing the foot and mouth disease virus 2A sequence confer efficient bicistronic gene expression in cultured cells and rat substantia nigra neurons. *Gene Ther* 2001; 8(11): 864-873.

Furuya N, Yu J, Byfield M, Pattingre S, Levine B. The evolutionarily conserved domain of Beclin 1 is required for Vps34 binding, autophagy, and tumor suppressor function. *Autophagy* 2005;1(1): 46-52.

Gasparini G, Harris AL. Clinical importance of the determination of tumor angiogenesis in breast carcinoma: much more than a new prognostic tool. *J Clin Oncol* 1995; 13(3): 765-782.

Gogvadze V, Orrenius S, Zhivotovsky B. Mitochondria in cancer cells: what is so special about them? *Trends Cell Biol* 2008; 18(4): 165-173.

Gozuacik D, Kimchi A. Autophagy as a cell death and tumor suppressor mechanism. *Oncogene* 2004; 23(16): 2891-2906.

Gu M, Cooper J, Taanman J, Schapira A. Mitochondrial DNA transmission of the mitochondrial defect in Parkinson's disease. *Ann Neurol* 1998; 44(2): 177-186.

Gwinn DM, Shackelford DB, Egan DF, Mihaylova MM, Mery A, Vasquez DS, Turk BE, Shaw RJ. AMPK phosphorylation of raptor mediates a metabolic checkpoint. *Mol Cell* 2008; 30(2): 214-226.

Hait WN, Jin S, Yang JM. A matter of life or death (or both): understanding autophagy in cancer. *Clin Cancer Res* 2006; 12(7): 1961-1965.

Huang H, Li F, Alvarez RA, Ash JD, Anderson RE. Downregulation of ATP synthase subunit-6, cytochrome c oxidase-III, and NADH dehydrogenase-3 by bright cyclic light in the rat retina. *Invest Ophthalmol Vis Sci* 2004; 45(8): 2489-2496.

Huber BE, Richards CA, Krenitsky TA. Retroviral-mediated gene therapy for the treatment of hepatocellular carcinoma: an innovative approach for cancer therapy. *Proc Natl Acad Sci USA* 1991; 88(18): 8039-8043.

Hunter T. Oncoprotein networks. *Cell* 1997; 88(3): 333-346.

Hwang SK, Kwon JT, Park SJ, Chang SH, Lee ES, Chung YS, Beck GR Jr, Lee KH, Piao L, Park J, Cho MH. Lentivirus-mediated carboxyl-terminal modulator protein gene transfection via aerosol in lungs of K-ras null mice. *Gene Ther* 2007; 14(24): 1721-1730.

Hwang SK, Lim HT, Minai-Tehrani A, Lee ES, Park J, Park SB, Bbeck GR Jr, Cho MH.

Repeated aerosol delivery of carboxyl-terminal modulator protein suppresses tumor in the lungs of K-ras^{LA1} mice. *Am J Respir Crit Care Med* 2009; 179(12): 1131-1140.

Hwang SK, Minai-Tehrani A, Yu KN, Chang SH, Kim JE, Lee KH, Park J, Beck GR Jr, Cho MH. Carboxyl-terminal modulator protein induces apoptosis by regulating mitochondrial function in lung cancer cells. *Int J Oncol* 2011; 40(5): 1515-1524.

Hwang SK, Piao L, Lim HT, Minai-Tehrani A, Yu KN, Ha YC, Chae CH, Lee KH, Beck GR, Park J, Cho MH. Suppression of lung tumorigenesis by leucine zipper/EF hand-containing transmembrane-1. *PLoS One* 2010; 5(9): e12535.

Jiang HL, Xu CX, Kim YK, Arote R, Jere D, Lim HT, Cho MH, Cho CS. The suppression of lung tumorigenesis by aerosol-delivered folate–chitosan-graft-polyethylenimine/Akt1 shRNA complexes through the Akt signaling pathway. *Biomaterials* 2009;30: 5844-5852.

Jin H, Xu CX, Kim HW, Chung YS, Shin JY, Chang SH, Park SJ, Lee ES, Hwang SK, Kwon JT, Minai-Tehrani A, Woo M, Noh MS, Youn HJ, Kim DY, Yoon BI, Lee KH, Kim TH, Cho CS, Cho MH. Urocanic acid-modified chitosan-mediated PTEN delivery via aerosol suppressed lung tumorigenesis in K-ras(LA1) mice. *Cancer Gene Ther* 2008; 15(5): 275-283.

Jung CH, Jun CB, Ro SH, Kim YM, Otto NM, Cao J, Kundu M, Kim DH. ULK-Atg13-FIP200 complexes mediate mTOR signaling to the autophagy machinery. *Mol Biol Cell* 2009; 20(7): 1992-2003.

Jung CH, Ro SH, Cao J, Otto NM, Kim DH. mTOR regulation of autophagy. *FEBS Lett* 2010; 584(7): 1287-1295.

Kim JH, Minai-Tehrani A, Kim YK, Shin JY, Hong SH, Kim HJ, Lee HD, Chang SH, Yu KN, Bang YB, Cho CS, Yoon TJ, Yu DY, Jiang HL, Cho MH. Suppression of tumor growth in H-ras12V liver cancer mice by delivery of programmed cell death protein 4 using galactosylated poly (ethylene glycol)-chitosan-graft-spermine. *Biomaterials* 2012; 33(6): 1894-1902.

Kim KW, Moretti L, Lu B. M867, a novel selective inhibitor of caspase-3 enhances cell death and extends tumor growth delay in irradiated lung cancer models. *PLoS ONE* 2008; 3(5): e2275.

Kim KW, Moretti L, Mitchell LR, Jung DK, Lu B. Combined Bcl-2/mammalian target of rapamycin inhibition leads to enhanced radiosensitization via induction of apoptosis and autophagy in non-small cell lung tumor xenograft model. *Clin Cancer Res* 2009; 15(19): 6096-6105.

Klump H, Schiedlmeier B, Vogt B, Ryan M, Ostertag W, Baum C. Retroviral vector-mediated expression of HoxB4 in hematopoietic cells using a novel coexpression strategy. *Gene Ther* 2001; 8(10): 811-817.

Kondo Y, Kanzawa T, Sawaya R, Kondo S. The role of autophagy in cancer development and response to therapy. *Nat Rev Cancer* 2005;5: 726-734.

Kota J, Chivukula RR, O'Donnell KA, Wentzel EA, Montgomery CL, Hwang HW, Chang

TC, Vivekanandan P, Torbenson M, Clark KR, Mendell JR, Mendell JT. Therapeutic microRNA delivery suppresses tumorigenesis in a murine liver cancer model. *Cell* 2009; 137(6): 1005-1017.

Kuma A, Matsui M, Mizushima N. LC3, an autophagosome marker, can be incorporated into protein aggregates independent of autophagy: caution in the interpretation of LC3 localization. *Autophagy* 2007;3(4): 323-328.

Lawrence TS, Chang EY, Hahn TM, Hertel LW, Shewach DS. Radiosensitization of pancreatic cancer cells by 2′, 2′-difluoro-2′-deoxycytidine. *Int J Radiat Oncol Biol Phys* 1996; 34(4): 867-872.

Lemasters JJ, Nieminen AL, Qian T, Trost LC, Elmore SP, Nishimura Y, Crowe RA, Cascio WE, Bradham CA, Brenner DA, Herman B. The mitochondrial permeability transition in cell death: a common mechanism in necrosis, apoptosis and autophagy. *Biochim Biophys Acta* 1998;1366(1-2):177-196.

Li P, Nijhawan D, Budihardjo I, Srinivasula SM, Ahmad M, Alnemri ES, Wang X. Cytochrome c and dATP-dependent formation of Apaf-1/caspase-9 complex initiates an apoptotic protease cascade. *Cell* 1997; 91(4): 479-489.

Li S, Huang L. Nonviral gene therapy: Promises and challenges. *Gene Ther* 2000; 7(1): 31-34.

Liang C, Feng P, Ku B, Dotan I, Canaani D, Oh BH, Jung JU. Autophagic and tumour suppressor activity of a novel beclin1-binding protein UVRAG. *Nat Cell Biol* 2006;

8(7): 688-698.

Lockshin RA, Zakeri Z. Apoptosis, autophagy, and more. *Int J Biochem Cell Biol* 2004;36(12): 2405-2419.

Lockshin RA, Zakeri Z. Caspase-independent cell death? *Oncogene* 2004;23(16):2766-2773

Lundstrom K, Boulikas T. Viral and non-viral vectors in gene therapy: technology development and clinical trials. *Technol Cancer Res Treat* 2003; 2(5): 471-486.

Maeda K, Kang SM, Onoda N, Ogawa M, Sawada T, Nakata B, Kato Y, Chung YS, Sowa M. Expression of p53 and vascular endothelial growth factor associated with tumor angiogenesis and prognosis in gastric cancer. *Oncology* 1998; 55(6): 594-599.

Maira SM, Galetic I, Brazil DP, Kaech S, Ingley E, Thelen M, Hemmings BA. Carboxyl-terminal modulator protein (CTMP), a negative regulator of PKB/Akt and v-Akt at the plasma membrane. *Science* 2001; 294(5541): 374-380.

Maiuri MC, Tasdemir E, Criollo A, Morselli E, Vicencio JM, Carnuccio R, Kroemer G. Control of autophagy by oncogenes and tumor suppressor genes. *Cell Death Differ* 2008; 16(1): 87-93.

Maiuri MC, Zalckvar E, Kimchi A, Kroemer G. Self-eating and self-killing: Crosstalk between autophagy and apoptosis. *Nat Rev Mol Cell Biol* 2007; 8(9): 741-752.

Marzo I, Brenner C, Zamzami N, Jürgensmeier JM, Susin SA, Vieira HLA, Prévost MC,

Xie Z, Matsuyama S, Reed JC. Bax and adenine nucleotide translocator cooperate in the mitochondrial control of apoptosis. *Science* 1998;281(5385): 2027-2031.

Marzo I, Brenner C, Zamzami N, Jürgensmeier JM, Susin SA, Vieira HL, Prévost MC, Xie Z, Matsuyama S, Reed JC, Kroemer G. Bax and adenine nucleotide translocator cooperate in the mitochondrial control of apoptosis. *Science* 1998; 281(5385): 2027-2031.

McLachlin JR, Mittereder N, Daucher MB, Kadan M, Eglitis MA. Factors affecting retroviral vector function and structural integrity. *Virology* 1993; 195(1): 1-5.

Miller DW, Graulich W, Karges B, Stahl S, Ernst M, Ramaswamy A, Sedlacek HH, Müller R, Adamkiewicz J. Elevated expression of endoglin, a component of the TGF-β-receptor complex, correlates with proliferation of tumor endothelial cells. *Int J Cancer* 1999; 81(4): 568-572.

Moretti L, Kim KW, Jung DK, Willey CD, Lu B. Radiosensitization of solid tumors by Z-VAD, a pan-caspase inhibitor. *Mol Cancer Ther* 2009; 8(5): 1270-1279.

Motoshima H, Goldstein BJ, Igata M, Araki E. AMPK and cell proliferation–AMPK as a therapeutic target for atherosclerosis and cancer. *J Physiol* 2006; 574(1): 63-71.

Nelson DA, White E. Exploiting different ways to die. *Genes Dev* 2004;18(11):1223-1226.

Newmeyer DD, Ferguson-Miller S. Mitochondria: releasing power for life and unleashing

the machineries of death. *Cell* 2003; 112(4): 481-490.

Niu G, Wright KL, Huang M, Song L, Haura E, Turkson J, Zhang S, Wang T, Sinibaldi D, Coppola D, Heller R, Ellis LM, Karras J, Bromberg J, Pardoll D, Jove R, Yu H. Constitutive Stat3 activity up-regulates VEGF expression and tumor angiogenesis. *Oncogene* 2002; 21(13): 2000-2008.

Parcellier A, Tintignac LA, Zhuravleva E, Cron P, Schenk S, Bozulic L, Hemmings BA. Carboxy-Terminal Modulator Protein (CTMP) is a mitochondrial protein that sensitizes cells to apoptosis. *Cell Signal* 2009; 21(4): 639-650.

Parkin DM, Bray FI, Devesa SS. Cancer burden in the year 2000: The global picture. *Eur J Cancer* 2001; 37(suppl8): S4-66.

Parr EL, Tung HN, Parr MB. Apoptosis as the mode of uterine epithelial cell death during embryo implantation in mice and rats. *Biol Reprod* 1987; 36(1): 211-225.

Pattingre S, Espert L, Biard-Piechaczyk M, Codogno P. Regulation of macroautophagy by mTOR and Beclin 1 complexes. *Biochimie* 2008; 90(2): 313-323.

Perkins CL, Fang G, Kim CN, Bhalla KN. The role of Apaf-1, caspase-9, and bid proteins in etoposide-or paclitaxel-induced mitochondrial events during apoptosis. *Cancer Res* 2000; 60(6): 1645-1653.

Phillips HS, Kharbanda S, Chen R, Forrest WF, Soriano RH, Wu TD, Misra A, Nigro JM, Colman H, Soroceanu L, Williams PM, Modrusan Z, Feuerstein BG, Aldape K.

Molecular subclasses of high-grade glioma predict prognosis, delineate a pattern of disease progression, and resemble stages in neurogenesis. *Cancer Cell* 2006; 9(3): 157-173.

Piao L, Li Y, Kim SJ, Sohn KC, Yang KJ, Park KA, Byun HS, Won M, Hong J, Hur GM, Seok JH, Shong M, Sack R, Brazil DP, Hemmings BA, Park J. Regulation of OPA1-mediated mitochondrial fusion by leucine zipper/EF-hand-containing transmembrane protein-1 plays a role in apoptosis. *Cell Signal* 2009; 21(5): 767-777.

Plum SM, Holaday JW, Ruiz A, Madsen JW, Fogler WE, Fortier AH. Administration of a liposomal FGF-2 peptide vaccine leads to abrogation of FGF-2-mediated angiogenesis and tumor development. *Vaccine* 2000; 19(9): 1294-1303.

Pouyssegur J, Dayan F, Mazure NM. Hypoxia signalling in cancer and approaches to enforce tumour regression. *Nature* 2006; 441(7092): 437-443.

Rabinowitz JE, Samulski J. Adeno-associated virus expression systems for gene transfer. *Curr Opin Biotechnol* 1998; 9(5): 470-475.

Rajawat YS, Hilioti Z, Bossis I. Aging: central role for autophagy and the lysosomal degradative system. *Ageing Res Rev* 2009;8(3): 199-213.

RCR. Radiotherapy Dose-Fractionation: Lung Cancer. London: The Royal College of Radiologists 2006; 43-48.

Rivière I, Brose K, Mulligan RC. Effects of retroviral vector design on expression of

human adenosine deaminase in murine bone marrow transplant recipients engrafted with genetically modified cells. *Proc Natl Acad Sci USA* 1995; 92(15):6733-6737.

Roth JA, Nguyen D, Lawrence DD, Kemp BL, Carrasco CH, Ferson DZ, Hong WK, Komaki R, Lee JJ, Nesbitt JC, Pisters KM, Putnam JB, Schea R, Shin DM, Walsh GL, Dolormente MM, Han CI, Martin FD, Yen N, Xu K, Stephens LC, McDonnell TJ, Mukhopadhyay T, Cai D. Retrovirus-mediated wild-type p53 gene transfer to tumors of patients with lung cancer. *Nat Med* 1996; 2(9): 985-991.

Sarbassov DD, Guertin DA, Ali SM, Sabatini DM. Phosphorylation and regulation of Akt/PKB by the rictor-mTOR complex. *Science* 2005;307(5712):1098-1101.

Schapira A, Cooper J, Dexter D, Clark J, Jenner P, Marsden C. Mitochondrial complex I deficiency in Parkinson's disease. *J Neurochem* 1990; 54(3): 823-827

Schatten H, Lewis ML, Chakrabarti A. Spaceflight and clinorotation cause cytoskeleton and mitochondria changes and increases in apoptosis in cultured cells. *Acta Astronautica* 2001; 49(3-10); 399-418.

Seghezzi G, Patel S, Ren CJ, Gualandris A, Pintucci G, Robbins ES, Shapiro RL, Galloway AC, Rifkin DB, Mignatti P. Fibroblast growth factor-2 (FGF-2) induces vascular endothelial growth factor (VEGF) expression in the endothelial cells of forming capillaries: an autocrine mechanism contributing to angiogenesis. *J Cell Biol* 1998; 141(7): 1659-1673.

Shintani T, Klionsky DJ. Autophagy in health and disease: A double-edged sword.

Science 2004; 306(5698): 990-995.

Suen DF, Norris KL, Youle RJ. Mitochondrial dynamics and apoptosis. *Gene Dev* 2008; 22(12): 1577-1590.

Sui L, Dong Y, Ohno M, Watanabe Y, Sugimoto K, Tokuda M. Survivin expression and its correlation with cell proliferation and prognosis in epithelial ovarian tumors. *Int J Oncol* 2002; 21(2): 315-320.

Sun Y, Liu JH, Jin L, Lin SM, Yang Y, Sui YX, Shi H. Over-expression of the Beclin1 gene upregulates chemosensitivity to anti-cancer drugs by enhancing therapy-induced apoptosis in cervix squamous carcinoma CaSki cells. *Cancer Lett* 2010; 294(2): 204-210.

Szymczak AL, Vignali DAA. Development of 2A peptide-based strategies in the design of multicistronic vectors. *Expert Opin Biol Th* 2005; 5(5): 627-638.

Tanaka K, Babic I, Nathanson D, Akhavan D, Guo D, Gini B, Dang J, Zhu S, Yang H, De Jesus J, Amzajerdi AN, Zhang Y, Dibble CC, Dan H, Rinkenbaugh A, Yong WH, Vinters HV, Gera JF, Cavenee WK, Cloughesy TF, Manning BD, Baldwin AS, Mischel PS. Oncogenic EGFP signaling activates an mTORC2-NFkB pathway that promotes chemotherapy resistance. *Cancer Discov* 2011; 1(6): 524-538.

Thun MJ, DeLancey JO, Center MM, Jemal A, Ward EM. The global burden of cancer: priorities for prevention. *Carcinogenesis* 2010; 31(1): 100-110.

Trichas G, Begbie J, Srinivas S. Use of the viral 2A peptide for bicistronic expression in transgenic mice. *BMC Biol* 2008; 6(1): 40.

Wang ZH, Xu L, Duan ZL, Zeng LQ, Yan NH, Peng ZL. Beclin 1-mediated macroautophagy involves regulation of caspase-9 expression in cervical cancer HeLa cells. *Gynecol Oncol* 2007; 107(1): 107-113.

Wei Y, Sinha S, Levine B. Dual role of JNK-mediated phosphorylation of Bcl-2 in autophagy and apoptosis regulation. *Autophagy* 2008; 4(7): 949-951.

Wolter KG, Hsu YT, Smith CL, Nechushtan A, Xi XG, Youle RJ. Movement of Bax from the cytosol to mitochondria during apoptosis. *J Cell Biol* 1997; 139(5): 1281-1292.

Wong AK, Alfert M, Castrillon DH, Shen Q, Holash J, Yancopoulos GD, Chin L. Excessive tumor-elaborated VEGF and its neutralization define a lethal paraneoplastic syndrome. *Proc Natl Acad Sci USA* 2001; 98(13): 7481-7486.

Xiang X, Saha AK, Wen R, Ruderman NB, Luo Z. AMP-activated protein kinase activators can inhibit the growth of prostate cancer cells by multiple mechanisms. *Biochem Biophys Res Commun* 2004; 321(1): 161-167.

Xu CX, Jere D, Jin H, Chang SH, Chung YS, Shin JY, Kim JE, Park SJ, Lee YH, Chae CH, Lee KH, Beck GR Jr, Cho CS, Cho MH. Poly (ester amine)-mediated, aerosol-delivered Akt1 small interfering RNA suppresses lung tumorigenesis. *Am J Respir Crit Care Med* 2008; 178(1): 60-73.

Xu CX, Jin H, Shin JY, Kim JE, Cho MH. Roles of protein kinase B/Akt in lung cancer. *Front Biosci (Elite Ed)* 2010; 2: 1472-1484.

Xu L, Yee JK, Wolff J, Friedmann T. Factors affecting long-term stability of Moloney murine leukemia virus-based vectors. *Virology* 1989; 171(2): 331-341.

Yang ZJ, Chee CE, Huang S, Sinicrope FA. The role of autophagy in cancer: therapeutic implications. *Mol Cancer Ther* 2011; 10(9): 1533-1541.

Yoshimori T. Autophagy: paying Charon's toll. *Cell* 2007; 128(5): 833-836

Young JL, Dean DA. Nonviral gene transfer strategies for the vasculature. *Microcirculation* 2002; 9(1): 35-50.

Yu KN, Minai-Tehrani A, Chang SH, Hwang SK, Hong SH, Kim JE, Shin JY, Park SJ, Kim JH, Kwon JT, Jiang HL, Kang B, Kim D, Chae CH, Lee KH, Yoon TJ, Beck GR, Cho MH. Aerosol delivery of small hairpin osteopontin blocks pulmonary metastasis of breast cancer in mice. *PLoS ONE* 2010; 5(12):e15623.

Zalckvar E, Berissi H, Mizrachy L, Idelchuk Y, Koren I, Eisenstein M, Sabanay H, Pinkas-Kramarski R, Kimchi A. DAP-kinase-mediated phosphorylation on the BH3 domain of beclin1 promotes dissociation of beclin1 from Bcl-XL and induction of autophagy. *EMBO Rep* 2009; 10(3): 285-292.

Zeng Z, Sarbassov dos D, Samudio IJ, Yee KW, Munsell MF, Ellen Jackson C, Giles FJ, Sabatini DM, Andreeff M, Konopleva M. Rapamycin derivatives reduce mTORC2

signaling and inhibit AKT activation in AML. *Blood* 2007; 109(8): 3509-3512.

Zhu CQ, Shih W, Ling CH, Tsao MS. Immunohistochemical markers of prognosis in non-small cell lung cancer: a review and proposal for a multiphase approach to marker evaluation. *J Clin Pathol* 2006; 59(8): 790-800.

국문초록

세포자식증 및 세포자살기전을 이용한 폐암 및 간암의 유전자치료 증진 연구

신 지 영
서울대학교 수의과대학
수의학과 수의공중보건(독성학)전공

의료기술의 발달에도 불구하고 폐암과 간암은 조기진단에 어려움이 있는 장기로서, 전세계적으로 발생율과 이로 인한 사망률은 계속해 증가하고 있는 추세이다. 더욱이 암이라는 질병의 경우, 한가지 유전자 혹은 단백질의 변형에 의해 발생하는 것이 아니므로 명확한 치료효과를 기대하기에는 여러가지 어려움이 따르게 된다. 세포자식증은 세포의 생(生)과 사(死) 모두를 조절하는 현상으로, 본 논문에서는 세포자식증 조절 및 2A peptide cleavage sequence 도입 등을 통하여 세포사를 유도, 치료효율을 높이고 치료효과의 상승효과를 보고자 하였다.

첫번째로 세포자식증에서 중심적인 역할을 하는 beclin1 을 치료유전자로 선정하였다. 렌티바이러스벡터에 beclin1을 클로닝하여 폐암모델마우스인 K-

ras^{LA1} 의 폐에 자식증이 지속적으로 활성화될 수 있게끔 beclin1 의 반복적 흡입노출을 시도하였다. Beclin1 이 효율적으로 전달됨으로서 세포자식증 관련 단백질인 beclin1, LC3-II 가 증가하고, 라이소좀의 기능과 연관성이 있는 p62 가 감소하는 양상을 나타내었으며, 이로 인해 K-ras^{LA1}의 폐에서 관찰되는 암조직이 개수와 크기측면에서 모두 감소하였고, 악성선암종으로의 진행이 억제되는 병리학적 결과를 확인할 수 있었다. 또한 전자현미경상에서 암조직을 관찰하였을 때 세포자식증 전형적인 공포화가 다수 관찰되었으며, 추가적으로 세포항상성을 유지하는데 있어 중요한 역할을 하는 사립체의 비정상적인 형태가 확인되었다. 세포자살기전이 활성화되면 가장먼저 핵변화가 일어나게 되고 이를 보상하기 위해 세포내 사립체 갯수가 증가하게 되는데, beclin1 을 과발현시켰을 때에도 이러한 현상이 관찰되었다. 그러나 ATP 형성과정에 직접적으로 관여하여 사립체의 기능을 평가하는 기준이 되는 mitochondrial 12S RNA 의 양은 그 갯수와 반비례 하는 것으로 나타났다. 사립체 관련 세포자살기전에 관여하는 Bax, Apaf-1, c-PARP, cytochrome *c* 뿐만 아니라 TUNEL 양성세포가 유의적으로 증가하였고, 결과적으로 자식증 뿐만 아니라 세포자살 기전도 동시에 활성화되어 항암효과를 보임을 확인하였다.

두번째로 부작용을 최소화하기 위해 시행되는 낮은 용량의 방사선 치료법에서 대두되는 암세포의 내성획득의 측면에서 자식증이 관여함을 확인하였다. 부작용을 최소화 하기 위해 흉부특이적으로 분할방사선조사법

(2Gy, 5회)을 시행하고 자식증 조절 유전자인 beclin1 을 동시에 노출시켜 그 항암효과를 확인하였다. 그 결과 세포질 내의 세포자식증으로 인한 공포화, 세포자식증 관련 단백질인 beclin1, ATG5, LC3-II 발현의 증가가 확인되었다. 방사선과 beclin1 의 흡입노출은 세포자식증 활성에 핵심적인 역할을 하는 beclin1-bcl2 complex 를 분리시키고, 더 나아가 Akt1 의 인산화(serine473, threonine308)를 억제시킴을 확인하였다. 또한 mTORC1 의 raptor, mTORC2의 rictor 에도 영향을 주게 되어 지속적인 세포자식증의 활성화가 positive feedback 을 유도하여 Akt1-mTOR 신호전달체계를 추가적으로 억제시켜 항암효과를 극대화 시킴을 확인하였다.

세번째로 두가지 이상의 유전자를 동시에 같은 효율로 발현시키기 위한 방안으로 대두된 개념인 2A-peptide 를 도입하여 그 효율을 생체 내에서 확인하였다. 간특이적 전달체인 galactosylated-poly(ethylene glycol)-chitosan-graft-spermine(GPCS) 를 이용, 사립체 조절 유전자인 CTMP 와 LETM1 을 2A peptide 로 연결시켜 H-ras12V 간암모델마우스에 4주간 반복적용 시켰을 때에 성공적으로 2A-peptide cleavage 가 일어남을 확인하였다. 또한 간암조직의 세포가 변성단계에 머물며 간세포샘종 혹은 간세포암종으로의 진행이 억제됨을 병리학적 분석을 통해 관찰되었으며, 전자현미경상으로도 사립체 내의 크리스타의 형태가 비정상적으로 관찰됨과 동시에 핵막의 변화(톱니바퀴모양, 핵막의 붕괴 등)가 확인되었다. 이는 사립체 관련 세포자살기전 단백질인 apaf-1, bax, cytochrome *c* 증가 및 TUNEL 양성세포

증가를 통해 입증되었으며, 간세포암종에서 세포자살을 통한 치료 가능성을 시사하였다.

기존에 행해지는 항암치료의 부작용을 최소화하고, 그 치료효율은 높이는 방법을 개발하는 것이 중요하다. 암 치료효율을 방해하는 자식증을 조절하기 위해 beclin1 을 도입하고 현재 임상에서 사용되는 분할방사선요법을 병행하여 치료효율을 높힐 수 있음을 확인하였다. 또한 하나 이상의 유전자를 동시에 조절하는 2A-peptide cleavage sequence 로 LETM1 과 CTMP 를 연결시켜 간특이적인 유전자전달체 GPCS 를 이용하여 전달함으로서 그 상승효과를 확인하였다. 단순히 하나의 유전자 혹은 치료방법을 이용한 기존의 항암요법과 비교할 때, 부작용을 야기하는 기전으로의 개입과 2개 이상의 유전자를 동시에 조절할 수 있는 기술 개발이 앞으로의 유전자치료제 개발에 있어 중요한 접근법이 될 수 있을 것으로 기대한다.

Keywords : 세포자식증, 세포자살, 폐암, 간암, 유전자치료

Student Number : 2009-31055

Publications

Shin JY, Chung YS, Kang B, Jiang HL, Yu DY, Han KW, Chae CH, Moon JH, Jang G, Cho MH. Co-delivery of LETM1 and CTMP synergistically inhibits tumor growth in H-ras12V liver cancer model mice. Cancer Gene Ther (in press)

Minai-Tehrani A, Chang SH, Kwon JT, Hwang SK, Kim JE, **Shin JY**, Yu KN, Park SJ, Jiang HL, Kim JH, Hong SH, Kang B, Kim D, Chae CH, Lee KH, Beck GR Jr, Cho MH. Aerosol delivery of lentivirus-mediated O-glycosylation mutant osteopontin suppresses lung tumorigenesis in K-ras (LA1) mice. Cell Oncol (Dordr). 2012 Oct 16. [Epub ahead of print]

Islam MA, **Shin JY**, Firdous J, Park TE, Choi YJ, Cho MH, Yun CH, Cho CS. The role of osmotic polysorbitol-based transporter in RNAi silencing via caveolae-mediated endocytosis and COX-2 expression. Biomaterials. 2012 Dec;33(34):8868-8880.

Shin JY, Lim HT, Minai-Tehrani A, Noh MS, Kim JE, Kim JH, Jiang HL, Arote R, Kim DY, Chae C, Lee KH, Kim MS, Cho MH. Aerosol delivery of beclin1 enhanced the anti-tumor effect of radiation in the lungs of K-rasLA1 mice. J Radiat Res. 2012 Jul;53(4):506-515.

Chang SH, Hong SH, Jiang HL, Minai-Tehrani A, Yu KN, Lee JH, Kim JE, **Shin JY**, Kang B, Park S, Han K, Chae C, Cho MH. GOLGA2/GM130, cis-Golgi Matrix Protein, is a Novel Target of Anticancer Gene Therapy. Mol Ther. 2012 Nov;20(11):2052-2063.

Luu QP, **Shin JY**, Kim YK, Islam MA, Kang SK, Cho MH, Choi YJ, Cho CS. High Gene Transfer by the Osmotic Polysorbitol-Mediated Transporter through the Selective Caveolae Endocytic Pathway. Mol Pharm. 2012 Jun 28. [Epub ahead of print]

Hong SH, Kim JE, Kim YK, Minai-Tehrani A, **Shin JY**, Kang B, Kim HJ, Cho CS, Chae C, Jiang HL, Cho MH. Suppression of lung cancer progression by biocompatible glycerol triacrylate-spermine-mediated delivery of shAkt1. Int J Nanomedicine. 2012;7:2293-2306.

Minai-Tehrani A, Jiang HL, Kim YK, Chung YS, Yu KN, Kim JE, **Shin JY**, Hong SH, Lee JH, Kim HJ, Chang SH, Park S, Kang BN, Cho CS, Cho MH. Suppression of tumor growth in xenograft model mice by small interfering RNA targeting osteopontin delivery using biocompatible poly(amino ester). Int J Pharm. 2012 Jul 15;431(1-2):197-203.

Chang SH, Minai-Tehrani A, **Shin JY**, Park S, Kim JE, Yu KN, Hong SH, Hong CM, Lee KH, Beck GR Jr, Cho MH. Beclin1-induced autophagy abrogates radioresistance of lung cancer cells by suppressing osteopontin. J Radiat Res. 2012;53(3):422-432.

Guo DD, Hong SH, Jiang HL, Kim JH, Minai-Tehrani A, Kim JE, **Shin JY**, Jiang T, Kim YK, Choi YJ, Cho CS, Cho MH. Synergistic effects of Akt1 shRNA and paclitaxel-incorporated conjugated linoleic acid-coupled poloxamer thermosensitive hydrogel on breast cancer. Biomaterials. 2012 Mar;33(7):2272-2281.

Kim JH, Minai-Tehrani A, Kim YK, **Shin JY**, Hong SH, Kim HJ, Lee HD, Chang SH, Yu KN, Bang YB, Cho CS, Yoon TJ, Yu DY, Jiang HL, Cho MH. Suppression of tumor growth in H-ras12V liver cancer mice by delivery of programmed cell death protein 4 using galactosylated poly(ethylene glycol)-chitosan-graft-spermine. Biomaterials. 2012 Feb;33(6):1894-1902.

Minai-Tehrani A, Park YC, Hwang SK, Kwon JT, Chang SH, Park SJ, Yu KN, Kim JE, **Shin JY**, Kim JH, Kang B, Hong SH, Cho MH. Aerosol delivery of kinase-deficient Akt1 attenuates Clara cell injury induced by naphthalene in the lungs of dual luciferase mice. J Vet Sci. 2011 Dec;12(4):309-317.

Kim JE, **Shin JY**, Cho MH. Magnetic nanoparticles: an update of application for drug delivery and possible toxic effects. Arch Toxicol. 2012 May;86(5):685-700. Epub 2011 Nov 11. Review.

Islam MA, Yun CH, Choi YJ, **Shin JY**, Arote R, Jiang HL, Kang SK, Nah JW, Park IK, Cho MH, Cho CS. Accelerated gene transfer through a polysorbitol-based transporter mechanism. Biomaterials. 2011 Dec;32(36):9908-9924.

Yu KN, Minai-Tehrani A, Chang SH, Hwang SK, Hong SH, Kim JE, **Shin JY**, Park SJ, Kim JH, Kwon JT, Jiang HL, Kang B, Kim D, Chae CH, Lee KH, Yoon TJ, Beck GR, Cho MH. Aerosol delivery of small hairpin osteopontin blocks pulmonary metastasis of breast cancer in mice. PLoS One. 2010 Dec 22;5(12):e15623.

Kim JE, Lim HT, Minai-Tehrani A, Kwon JT, **Shin JY**, Woo CG, Choi M, Baek J, Jeong DH, Ha YC, Chae CH, Song KS, Ahn KH, Lee JH, Sung HJ, Yu IJ, Beck GR Jr, Cho

MH. Toxicity and clearance of intratracheally administered multiwalled carbon nanotubes from murine lung. J Toxicol Environ Health A. 2010;73(21-22):1530-1543.

Jiang HL, Lim HT, Kim YK, Arote R, **Shin JY**, Kwon JT, Kim JE, Kim JH, Kim D, Chae C, Nah JW, Choi YJ, Cho CS, Cho MH. Chitosan-graft-spermine as a gene carrier in vitro and in vivo. Eur J Pharm Biopharm. 2011 Jan;77(1):36-42.

Xu CX, Jin H, **Shin JY**, Kim JE, Cho MH. Roles of protein kinase B/Akt in lung cancer. Front Biosci (Elite Ed). 2010 Jun 1;2:1472-1484. Review.

Hwang SK, Minai-Tehrani A, Lim HT, **Shin JY**, An GH, Lee KH, Park KR, Kim YS, Beck GR Jr, Yang HS, Cho MH. Decreased level of PDCD4 (programmed cell death 4) protein activated cell proliferation in the lung of A/J mouse. J Aerosol Med Pulm Drug Deliv. 2010 Oct;23(5):285-293.

Xu CX, Jin H, Chung YS, **Shin JY**, Hwang SK, Kwon JT, Park SJ, Lee ES, Minai-Tehrani A, Chang SH, Woo MA, Noh MS, An GH, Lee KH, Cho MH. Low dietary inorganic phosphate affects the lung growth of developing mice. J Vet Sci. 2009 Jun;10(2):105-113.

Cho HS, Chang SH, Chung YS, **Shin JY**, Park SJ, Lee ES, Hwang SK, Kwon JT, Tehrani AM, Woo M, Noh MS, Hanifah H, Jin H, Xu CX, Cho MH. Synergistic effect of ERK inhibition on tetrandrine-induced apoptosis in A549 human lung carcinoma cells. J Vet Sci. 2009 Mar;10(1):23-28.

Jin H, Xu CX, Lim HT, Park SJ, **Shin JY**, Chung YS, Park SC, Chang SH, Youn HJ, Lee KH, Lee YS, Ha YC, Chae CH, Beck GR Jr, Cho MH. High dietary inorganic phosphate increases lung tumorigenesis and alters Akt signaling. Am J Respir Crit Care Med. 2009 Jan 1;179(1):59-68.

Xu CX, Jin H, Chung YS, **Shin JY**, Lee KH, Beck GR Jr, Palmos GN, Choi BD, Cho MH. Chondroitin sulfate extracted from ascidian tunic inhibits phorbol ester-induced expression of Inflammatory factors VCAM-1 and COX-2 by blocking NF-kappaB activation in mouse skin. J Agric Food Chem. 2008 Oct 22;56(20):9667-9675.

Xu CX, Jin H, Lim HT, Kim JE, **Shin JY**, Lee ES, Chung YS, Lee YS, Beck G Jr, Lee KH, Cho MH. High dietary inorganic phosphate enhances cap-dependent protein translation, cell-cycle progression, and angiogenesis in the livers of young mice. Am J Physiol Gastrointest Liver Physiol. 2008 Oct;295(4):G654-663.

Xu CX, Jere D, Jin H, Chang SH, Chung YS, **Shin JY**, Kim JE, Park SJ, Lee YH, Chae CH, Lee KH, Beck GR Jr, Cho CS, Cho MH. Poly(ester amine)-mediated, aerosol-delivered Akt1 small interfering RNA suppresses lung tumorigenesis. Am J Respir Crit Care Med. 2008 Jul 1;178(1):60-73.

Xu CX, Jin H, Chung YS, **Shin JY**, Woo MA, Lee KH, Palmos GN, Choi BD, Cho MH. Chondroitin sulfate extracted from the Styela clava tunic suppresses TNF-alpha-induced expression of inflammatory factors, VCAM-1 and iNOS by blocking Akt/NF-kappaB signal in JB6 cells. Cancer Lett. 2008 Jun 8;264(1):93-100.

Jin H, Xu CX, Kim HW, Chung YS, **Shin JY**, Chang SH, Park SJ, Lee ES, Hwang SK, Kwon JT, Minai-Tehrani A, Woo M, Noh MS, Youn HJ, Kim DY, Yoon BI, Lee KH, Kim TH, Cho CS, Cho MH. Urocanic acid-modified chitosan-mediated PTEN delivery via aerosol suppressed lung tumorigenesis in K-ras(LA1) mice. Cancer Gene Ther. 2008 May;15(5):275-283.

Jin H, Chang SH, Xu CX, **Shin JY**, Chung YS, Park SJ, Lee YS, An GH, Lee KH, Cho MH. High dietary inorganic phosphate affects lung through altering protein translation, cell cycle, and angiogenesis in developing mice. Toxicol Sci. 2007 Nov;100(1):215-223.